U.S. DEPARTMENT OF ENERGY

PNNL- 22041

Prepared for the U.S. Department of Energy
under Contract DE-AC05-76RL01830

Assessment of Strike of Adult Killer Whales by an OpenHydro Tidal Turbine Blade

Revision 2.1

TJ Carlson
JL Elster
ME Jones
BE Watson
AE Copping
M Watkins

R Jepsen
K Metzinger

November 2012

Pacific Northwest NATIONAL LABORATORY

Proudly Operated by Battelle *Since 1965*

DISCLAIMER

This report was prepared as an account of work sponsored by an agency of the United States Government. Neither the United States Government nor any agency thereof, nor Battelle Memorial Institute, nor any of their employees, makes **any warranty, express or implied, or assumes any legal liability or responsibility for the accuracy, completeness, or usefulness of any information, apparatus, product, or process disclosed, or represents that its use would not infringe privately owned rights**. Reference herein to any specific commercial product, process, or service by trade name, trademark, manufacturer, or otherwise does not necessarily constitute or imply its endorsement, recommendation, or favoring by the United States Government or any agency thereof, or Battelle Memorial Institute. The views and opinions of authors expressed herein do not necessarily state or reflect those of the United States Government or any agency thereof.

PACIFIC NORTHWEST NATIONAL LABORATORY
operated by
BATTELLE
for the
UNITED STATES DEPARTMENT OF ENERGY
under Contract DE-AC05-76RL01830

Printed in the United States of America

Available to DOE and DOE contractors from the
Office of Scientific and Technical Information,
P.O. Box 62, Oak Ridge, TN 37831-0062;
ph: (865) 576-8401
fax: (865) 576-5728
email: reports@adonis.osti.gov

Available to the public from the National Technical Information Service,
U.S. Department of Commerce, 5285 Port Royal Rd., Springfield, VA 22161
ph: (800) 553-6847
fax: (703) 605-6900
email: orders@ntis.fedworld.gov
online ordering: http://www.ntis.gov/ordering.htm

This document was printed on recycled paper.
(9/2003)

PNNL- 22041

Assessment of Strike of Adult Killer Whales by an OpenHydro Tidal Turbine Blade

Revision 2.0

TJ Carlson
JL Elster
ME Jones
R Jepsen[1]
K Metzinger[1]
BE Watson
AE Copping
M Watkins

November 2012

Prepared for
the U.S. Department of Energy
under Contract DE-AC05-76RL01830

Pacific Northwest National Laboratory
Richland, Washington 99352

[1] Sandia National Laboratories, Albuquerque, New Mexico.

Summary

Snohomish County Public Utility District No. 1 (SnoPUD) proposes to deploy two OpenHydro tidal turbines in Admiralty Inlet, Puget Sound. The fisheries service of the National Oceanic and Atmospheric Administration (NOAA Fisheries) has expressed concerns that the turbines may cause a risk for the highly endangered Southern Resident killer whale (SRKW) population if a whale is struck by an operating turbine. NOAA Fisheries is responsible for protecting the (fewer than 90) SRKWs under the *Endangered Species Act of 1973* and the *Marine Mammal Protection Act of 1972*. Because the SRKW numbers are so small, significant injury of a single animal could place the population in jeopardy.

The potential risk to a SRKW can be parsed into the probability that a whale would encounter a turbine, the probability that the encounter would injure the whale, and the severity of any injury. During a meeting with representatives of SnoPUD, OpenHydro, the U.S. Department of Energy (DOE), and NOAA Fisheries, participants agreed that the probability of a SRKW encountering a turbine by chance is negligibly small because the whales spent greater than 97% of their time in Admiralty Inlet in the top 30 m of water; the turbines are located at 55 m of depth, and the SRKW have highly evolved acoustic sensory capabilities that would help them detect the presence of a turbine. NOAA Fisheries expressed concerns over the potential severity of a strike on a SRKW, should it occur. Further, a SRKW may approach a turbine out of curiosity. A proposed solution was to conduct an estimate of the level of injury that might occur from an encounter between a turbine blade and a SRKW, which would allow NOAA Fisheries to determine the permitting requirements for the tidal project.

Pacific Northwest National Laboratory (PNNL) and Sandia National Laboratories (SNL) were tasked by DOE to carry out an analysis of the mechanics and biological consequences of strike of a SRKW by an OpenHydro turbine blade. The approach taken by the two laboratories was to 1) develop a scenario for the most severe strike of a SRKW, 2) determine the morphological and biomechanical properties of SRKW tissues that might be affected by a strike, 3) model the forces of a strike, and 4) estimate the potential effects on SRKW tissue and bone of a strike.

PNNL and SNL developed a worst-case exposure scenario for strike of a SRKW. SNL modeled a blunt edge turbine blade (based on proprietary design data obtained from OpenHydro) and calculated the force of blade impact on the head of an adult male SRKW weighing approximately 4000 kg. The adult SRKW was selected for the model because an adult has a large body mass where more of the energy in a blade strike will be absorbed by the whale's tissue rather than going into momentum transfer that would push the whale out of the path of the turbine blade. This scenario would maximize the risk of injury to the SRKW. Although a juvenile SRKW might intuitively be considered to be at greater risk of injury, because of its much smaller mass (~500 kg) more of the energy in the blade strike would go into momentum transfer, pushing the juvenile SRKW out of the path of the turbine's blades, leaving much less body mass available to damage tissue. The duct surrounding the OpenHydro turbines planned for Puget Sound are narrow, extending less than one meter from the face of the turbine, allowing even a small SRKW to back away from the turbine.

SNL built models of the turbine blades and their motion using specifications and data supplied by OpenHydro (Figure ES.1) and of an adult male SRKW using data available in the literature (Figure ES. 2).

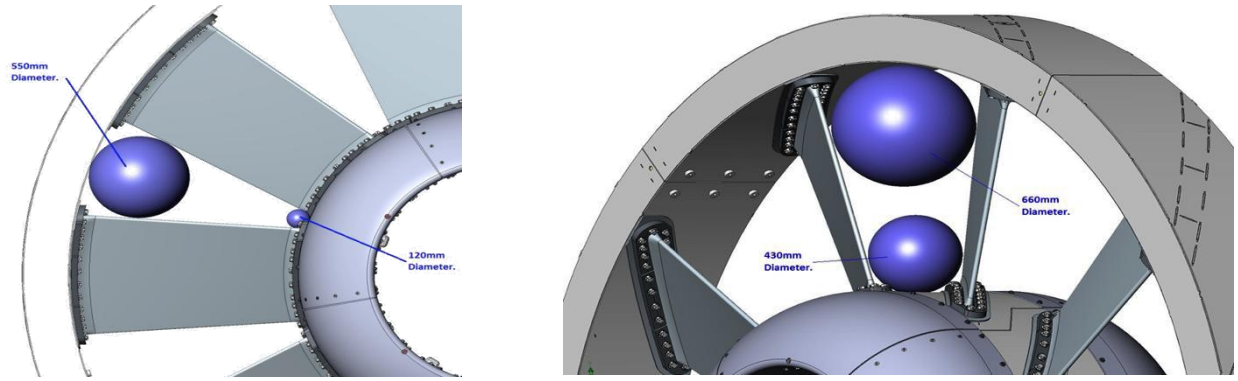

Figure ES.1. Drawings of the OpenHydro turbine blade assembly, as specified by OpenHydro, showing spacing of blade edges (left) and the spacing between blades (right). Also shown is the length of the blades (approximately 1.25 m) after accounting for the open hub of the blade assembly that has a diameter of 4.8 m.

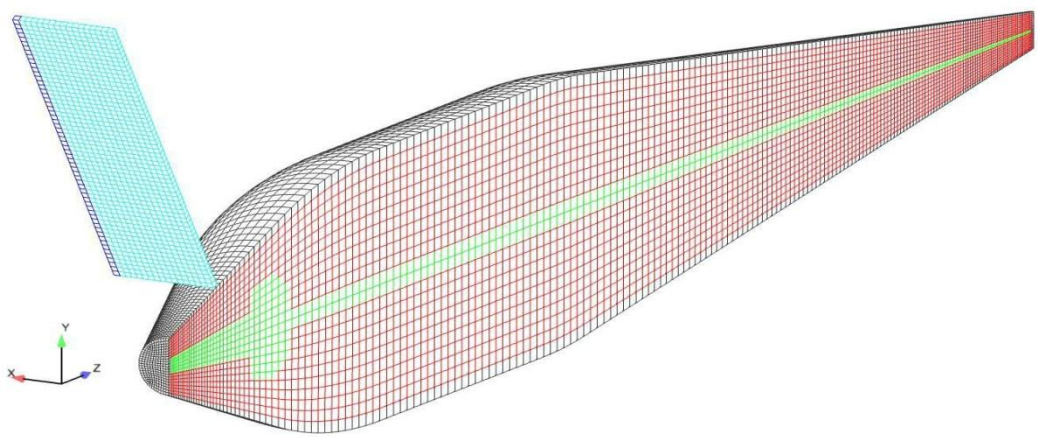

Figure ES. 2. The finite element mesh created for the model of the SRKW and the tidal turbine blade. The turbine is represented by a single blade. Due to the ducted turbine design, which encloses the tips of the turbine blades, and the spacing between blades, strike could conceivably occur on only the rostrum of a SRKW.

Recent NOAA publications provided appropriate SRKW swimming speeds of 1 m/s to 3 m/s for the type of encounter envisioned in this scenario. The modeling results showed maximum stresses (pressure) for turbine blade strike of the head of an adult male SRKW of about 2.350 MPa, with a strain (tissue elongation) of 73% for the most probable rotation speed of the turbine. Comparisons of other stress forces that can put the turbine strike (calculated to be 2.350 MPa) in context include: the stress of a baseball bat hitting a baseball pitched at 90 mph (72.98 MPa); the stress to a player's head from heading a soccer ball moving at 29 mph (.47 MPa). Although there are no publically accessible data that measure the stress of a ship striking a whale, it has been calculated that a 5000 metric ton ship moving 17 mph, where the bow of the ship strikes a .5 inch x 24 inch area of a whale, the stress would be 25.33 MPa, over 10 times the stress forces calculated for the turbine strike.

PNNL obtained data for the morphology and anatomy from computerized tomography (CT) scans of the head of an adult SRKW that died in 2002 (Figure ES.3). Information on the biomechanical properties of whale tissues was found in the scientific literature.

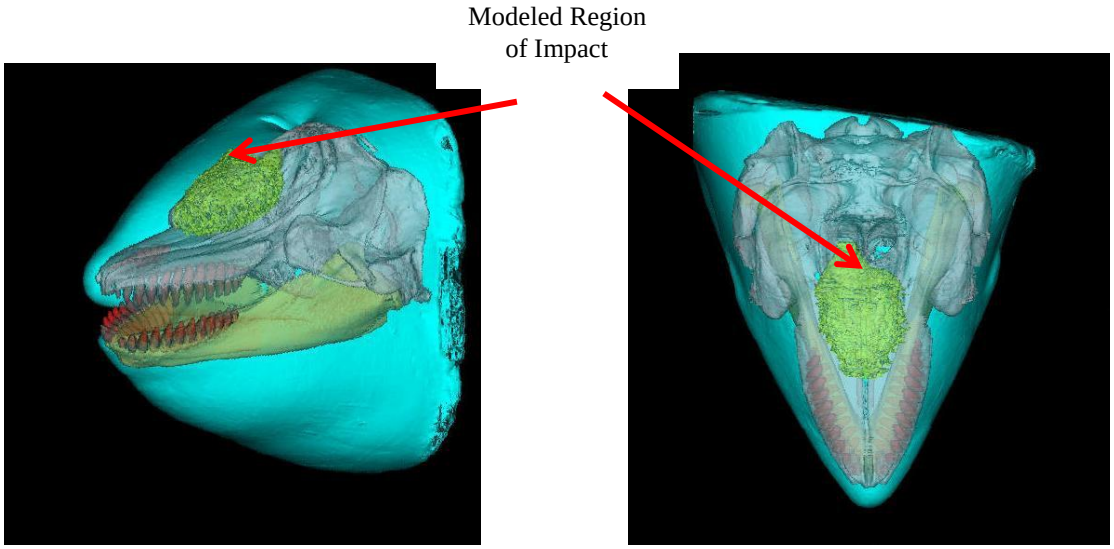

Figure ES.3. CT scan-based images of the head of an adult female SRKW from the side (left) and from top view (right). The teeth are shown in red, bone in light color, and the various soft tissues in other colors. The region of impact used for modeling purposes is indicated.

The adult killer whale for which CT scan data were available and the adult killer whale modeled were similar enough in size so that the available morphology and anatomy data from CT scans could be used in assessment of the probable injury to an adult killer whale caused by turbine blade strike. The tissues of concern included the skin of the whale, other soft tissue, and mandibular bone. Very little is known about the biomechanical properties of whale tissue under compression, particularly the skin, which functions to resist mechanical and other damage and to spread the force of an impact across a region that minimizes the stresses acting on underlying tissues; data that describes the biomechanical properties of the dorsal fin of a harbor porpoise under extension forces can be found in Hanson 2001. For the purposes of this analysis, several natural and synthetic rubber material properties were considered as the most appropriate surrogates for the SRKW dermal layer under compression.

Comparison of the maximum force acting on soft tissue and bone, estimated by SNL using the finite element models of the turbine blade and whale with the tissue biomechanics data developed by PNNL, provided the basis for assessment of probable injury to SRKW. The analysis found that the maximum levels of stress acting on whale tissue and bone corresponded to tissue response (strain) in the elastic range where whale tissue would be expected to return to their normal shape when the force of the turbine blade was removed without causing permanent change to the tissue. In addition, the stresses and strains estimated using the blade and whale models were well below the yield strength for similar material, including natural and synthetic rubber and human skin, by a factor of 3 or more.

PNNL examined the available literature on blunt force head trauma in marine mammals and interacted with marine veterinarians with experience in caring for injured animals and performing necropsies on animals found dead.

There is a paucity of data available on the biomechanics of SRKW tissues under compression, particularly skin, creating a challenge for estimating the potential effects of a turbine blade strike. The finite element modeling and engineering analysis carried out by SNL relies on the technical data provided by the turbine manufacturer and physical principles. The SRKW modeled in the finite element model was composed of a single layer of tissue, essentially a whale made entirely of blubber. The choice of this structure introduces a conservative element to the outcome, as the skin of marine mammals (particularly predatory animals such as SRKWs that use their heads to batter prey) is known to be stronger and more resistive to puncture and deformation. In the real world, the forces from a tidal turbine blade strike that might cause injury to the "all blubber" whale will cause less damage to the living animal. The scarcity of biomechanical data for compression deformation and puncture of the SRKW's skin led the PNNL researchers to seek adequate surrogates to estimate the likely outcome of a turbine blade strike. Natural and synthetic rubbers materials were deemed to be most similar (although somewhat more fragile) than SRKW skin. The lack of biomechanical compression measurements did not allow for calculations with which to modify the engineering analysis; rather these assessments of surrogate tissues further reinforced the concept that the assessment of potential harm to the SRKW from a tidal turbine strike is a conservative estimate.

The results of these analyses provide the following insights into the potential risk of encounter to a SRKW with an OpenHydro tidal turbine in Admiralty Inlet:

- PNNL/SNL analyses determined that a SRKW is not likely to experience significant tissue injury from impact by an OpenHydro turbine blade.
- If whale skin behaves similarly to the materials considered as surrogates for the upper dermal layers of whale skin, it is expected that in the case of a strike, whale skin tissue and the underlying soft tissue would deform, absorb the force of the strike, and return to normal condition The only published data on the strike pressure needed to fracture the mandibular bone (jawbone) of a cetacean comes from a North Atlantic right whale (NARW). Although the NARW is much larger than a SRKW and has a more massive mandibular, in the absence of other data, this analysis assumed that the SRKW mandibles have similar biomechanical properties to those of right whales. This assumption is considered to be appropriate as SRKWs are thought to have sturdy mandibles, based on the animals' observed behavior using their rostrums to batter prey animals and battle conspecifics. Applying this assumption, the highest stress predicted by the model (about 3.750 MPa) is highly unlikely to result in the fracture of a SRKW mandible. The mandible of an orca is partially hollow which could increase the vulnerability of the animal to damage; there are no data that will assist with this assessment at this time. The available literature and best professional judgment of marine veterinarians did not differ from the outcome of the analyses.

There are a number of areas in which the PNNL/SNL analysis could not provide insight:

- PNNL/SNL analyses could not provide insight into the potential for subtler changes to SRKWs from an encounter with the turbine, such as changes in behavior. Other scenarios that were discussed included a potential encounter of different life stages of the SRKW (neonate, juvenile, subadult, smaller adult female), as well as an encounter of other body parts with the turbine blade (fin, fluke,

ventral surface). None of these scenarios appeared to represent the curiosity-driven approach that formed the basis for concern (and hence drove this analysis), nor do they represent the "worst-case" scenario for momentum transfer (and hence the greatest potential for harm to the SRKW).

- PNNL/SNL analyses may help to inform, but do not adequately address or assess turbine interactions for other whales with other turbines.

The PNNL/SNL analyses were limited by the available time frame in which results were needed and focused on the mechanical response of whale tissues and bone to blade strike. Additional information on the biomechanical properties of marine mammal tissues and finite model refinements could help to further fine-tune this analysis. This analysis concentrated on the open center design specific to the OpenHydro turbine; the results may not be directly comparable to other turbine designs, but may help to inform similar analyses.

Acknowledgments

This study was conceived through the joint efforts of the U.S. Department of Energy (DOE), the National Oceanic and Atmospheric Administration (NOAA), Snohomish County PUD, OpenHydro, the University of Washington Northwest National Marine Renewable Energy Center (UW–NNMREC), Pacific Northwest National Laboratory (PNNL), and Sandia National Laboratories (SNL). Understanding the potential severity of strike from an OpenHydro turbine blade on a Southern Resident killer whale (SRKW) in Admiralty Inlet, Puget Sound, is a necessary step in the responsible deployment of tidal turbines in these waters.

Rich Jepsen and Kurt Metzinger SNL undertook the engineering analysis, based on turbine specifications supplied by OpenHydro, and tidal velocities supplied by UW–NNMREC. Sandia analyses were passed on to the biomechanical analysis team at PNNL.

Tom Carlson, Mike Watkins, and their team at PNNL examined the physiological and biomechanical properties of SRKWs and analyzed the likely effect of impacts, drawing from the engineering analysis.

Dr. Ted Cranfield at the University of California–Santa Cruz kindly supplied the team with CT scans of the head of a SRKW.

Dr. William McLellan of University of North Carolina–Wilmington, Dr. Steven Raverty of the province of British Columbia and University of British Columbia, Dr. Regina Campbell-Malone of Johns Hopkins University, Dr. James McBain of SeaWorld, and Dr. Joe Gaydos of the SeaDoc Society shared their expertise and experience in marine mammal injury and mortality.

Acronyms and Abbreviations

CT	computerized tomography
cm	centimeter(s)
DOE	U.S. Department of Energy
HIC	head injury criteria
in.	inch(es)
kg	kilogram(s)
kPa	kilopascal(s)
m	meter(s)
mm	millimeter(s)
m/s	meter(s) per second
MPa	megapascal(s)
NOAA	National Oceanic and Atmospheric Administration
PNNL	Pacific Northwest National Laboratory
SNL	Sandia National Laboratories
SnoPUD	Snohomish County Public Utility District No. 1
SRKW	Southern Resident killer whale
UW–NNMREC	University of Washington–Northwest National Marine Renewable Energy Center

Contents

Summary iii
Acknowledgments ix
Acronyms and Abbreviations x
1.0 Introduction 1
2.0 Engineering Analysis of Impact 3
2.1 Geometry and Operational Characteristics of OpenHydro Turbines 3
2.1.1 Turbine Design and Blade Material Properties 3
2.1.2 Rotor Rotation Rates and Blade Speed 5
2.2 Blade Impact Scenarios and Physical Characteristics of a SRKW 6
2.2.1 Blade Impact Scenarios 6
2.2.2 Material Properties for SRKW 9
2.3 Analysis with Finite Element Model 10
2.3.1 Model Setup 10
2.3.2 Impact Analysis Results 13
2.3.3 Including Forward Velocity of SRKW 18
3.0 Biological Assessment of Consequences of Impact 19
3.1 Whale Head Morphology 19
3.2 Tissue Models and Biomechanical Data 22
3.3 Biomechanics of Human Skin 27
3.4 Consequence of Turbine Blade Impact on Whale Tissue 28
4.0 Additional Information to Inform Strike Modeling: Blunt Force Trauma and Real-World Experience 30
4.1 Blunt Force Trauma Research 30
4.2 Assessments from Marine Veterinarians 31
5.0 Discussion and Conclusions 33
5.1 Interpretation of Engineering and Biomechanical Analyses 33
5.2 Uncertainty of Analyses Outcomes 33
5.3 Additional Information to Inform Analyses 35
5.4 Next Steps 35
5.5 Conclusion 36
6.0 References 37

Figures

Figure 1. Front view of blade with spacing dimensions of blade edges 4
Figure 2. Isometric view with spacing between blade faces 4
Figure 3. Angles between inner blade edges 4
Figure 4. Angles between outer blade edges 4
Figure 5. Probability distribution of velocity at blade tip. At low tidal velocity (26% of the time), the blade is stationary (not shown here) 5
Figure 6. Basic dimensions measured for SRKW (Durban et al. 2009) 6
Figure 7. Maximum dimensions reported for an adult male SRKW 6
Figure 8. Plot of probability distribution for velocity at a location of 0.4 m from the tip of the blade 7
Figure 9. "Maximum velocity" SRKW and blade impact scenario schematic 8
Figure 10. Stress-strain curve for whale blubber (Soldevilla et al. 2005, Figure 7) 10
Figure 11. Finite element mesh 12
Figure 12. Finite element mesh, impact region 12
Figure 13. Impact force as a function of time for different blade speeds 14
Figure 14. Strain, standard blade, 1 m/s at peak load 15
Figure 15. Pressure, standard blade, 1 m/s at peak load 15
Figure 16. Strain, standard blade, 3 m/s at peak load 16
Figure 17. Pressure, standard blade, 3 m/s at peak load 16
Figure 18. Maximum strain (log strain) and stress versus impact velocity 17
Figure 19. A sagittal CT scan of the head of an adult killer whale. Bone is shown as pink with the lower mandible in orange, teeth as red, voids are black, and other tissues in various other colors. Portions of the upper mandible of the whale's jaw and a cross section through the whale's skull are clear 20
Figure 20. CT scan of a transverse slice through the head of a killer whale approximately 40 cm from the tip of the whale's snout. The red line identifies a transect through the slice where CT scan image intensity values were sampled. In this figure, bone is white, voids are black, and other tissues are gray. 21
Figure 21. Intensity values along a vertical transect through a transverse slice of CT scan data for the head of a killer whale 22
Figure 22. Description of material toughness in the context of stress-strain dynamics 24
Figure 23. Structural advantages of a vertical fiber orientation within the epidermis. Fibers provide resistance to: (a) indentation and (b) lateral abrasion. (Winn 2006) 25
Figure 24. Examples of stress-strain characteristics for some manmade elastomers (*The Physics of Rubber*, http://www.allsealsinc.com/allseals/Orings/or13.htm) 26
Figure 25. Relationship between stress and strain for human skin showing true stress (unfilled squares), elastic (diamond symbols), and viscous (filled squares) components (after Silver et al. 2001, Figure 2) 28

Tables

Table 1. Resultant SRKW impact velocity for 5-m/s blade velocity combined with a range of forward velocities 9
Table 2. Elastic moduli (kPa) for several whale tissue types (Soldevilla et al. 2005, Table 4) 9
Table 3. Material properties used for analysis 13
Table 4. Peak stress and strain from computational simulations 14
Table 5. Peak stress and strain from Equations (1) and (2) 17
Table 7. Comparative epidermal ranges reported for baleen whale species (Winn 2006, Table 1). 24
Table 8. Properties of various elastomers (Schaefer 2009, Table 33.2) 26
Table 9. Mechanical properties of various elastomers (http://www.matbase.com and http://www.matweb.com/) 27
Table 10. Level of certainty associated with each input to the engineering and biomechanical analyses 34

1.0 Introduction

Snohomish County Public Utility District No. 1 (SnoPUD) has proposed to deploy two OpenHydro tidal turbines in Admiralty Inlet, Puget Sound. Due to the presence of the Southern Resident killer whale (SRKW) population (listed as an endangered species under the Endangered Species Act) in Puget Sound and Admiralty Inlet, the National Oceanic and Atmospheric Administration (NOAA Fisheries) has expressed concern that the turbines may cause a risk to the SRKW population. Because SRKW spend 97% of their time within the top 30 m of the water column and dive to the turbine depth (approximately 55 m) only to feed, the chance of a SRKW encountering a tidal turbine is negligibly small (Baird 2003). Further, it is possible a SRWK may approach the turbine out of curiosity. Due to their endangered status, there are concerns regarding the potential severity of a strike on a SRKW, should it occur. Because the SRKW numbers are so small, significant injury of a single animal could place the population in jeopardy.

To resolve this issue, Pacific Northwest National Laboratory (PNNL) and Sandia National Laboratories (SNL) were tasked by the U.S. Department of Energy (DOE) to carry out an analysis of the mechanics and biological consequences of a tidal turbine blade strike on a SRKW. In doing so, the potential level of injury from such an interaction can be estimated and used to inform NOAA Fisheries on how to proceed with the permitting process for the tidal energy project.

The approach taken was as follows:

1. PNNL and SNL developed a scenario for the most severe strike of a SRKW, consisting of a large male SRKW inspecting the tidal turbine out of curiosity, by placing its rostrum between the blades.
2. SNL analyzed the geometry, mass, material properties, and speed characteristics of the tidal turbines and calculated the amount of force a tidal turbine blade is capable of creating. This force calculation was coupled with the dimensions and material properties of an adult SRKW weighing approximately 4000 kg to develop a model simulation of a blade impact on the head of an adult SRKW.
3. PNNL used a computerized tomography (CT) scan of an adult SRKW head, similar in size to the hypothetical SRKW used in the engineering analysis, to understand the morphology and anatomy of a SRKW head. Scientific literature and surrogate synthetic rubber materials were used to support estimates of the biomechanical properties of whale skin and soft tissues and to determine how these tissues resist mechanical damages by spreading force across the region of impact. This analysis was used to estimate the level of injury that might occur from an encounter between a turbine blade and a SRKW.
4. By combining the maximum force calculations of the tidal turbine blade acting on the SRKW soft tissue and bone with SRKW tissue biomechanics and head anatomy data, PNNL and SNL were able to estimate the potential effects of an encounter between a SRKW and a tidal turbine blade.
5. PNNL examined the scientific literature on blunt force trauma to determine whether there are appropriate analogues to effects of a tidal turbine blade on the head region of a SRKW.
6. PNNL sought real-world examples of strike on the head region of SRKWs or other marine mammals through discussions with marine veterinarians who routinely treat or research injured marine mammals. The purpose of the real-world examples was to provide a semi-quantitative validation of the modeling results.

The engineering studies, biomechanical analyses, blunt force head trauma literature review, and model validation effort are discussed and synthesized in the discussion/conclusion section of this report to demonstrate how these analyses were used to provide information that may assist NOAA Fisheries in their permitting decisions for the tidal energy project in Admiralty Inlet, Washington. This strike analysis relies heavily on modeling the forces exerted from a moving turbine blade and estimating the biomechanics of SRKW tissues; each step in the analysis process introduces a level of uncertainty into the result, stemming largely from the uncertainty surrounding the available input data. A brief analysis of the level of accuracy associated with each portion of the analysis is provided in the discussion/conclusion section of this report as well.

2.0 Engineering Analysis of Impact

This section outlines the engineering analysis performed by SNL to determine the stresses on a SRKW from a potential impact with a tidal turbine blade. The analysis entailed determining the relevant geometry, mass, material, and speed characteristics of the OpenHydro turbine, rotor, and blade. SRKW dimensions and material properties were determined along with possible impact scenarios for the study.

2.1 Geometry and Operational Characteristics of OpenHydro Turbines

Relevant information was gathered on the geometry and operation of the OpenHydro turbines to be deployed in Puget Sound by:

- Obtaining design drawings with the necessary details of the blade assembly and rotor for the OpenHydro turbine. Key details include the number, location, shape, and angle of the blades, with dimensions of the leading blunt edge of the blades.
- Obtaining information on the materials and construction detail of the turbine blade assembly and rotor to compute blade mass and other physical properties.
- Obtaining information on the operating characteristics of the turbine including revolutions per minute/blade speed at the range of tidal flows expected in Admiralty Inlet.

All of the above data were supplied by OpenHydro with assistance from the University of Washington –Northwest National Marine Renewable Energy Center (UW–NNMREC) and are summarized below. It should be noted that designs are not finalized, and some parameters such as materials and moment of inertia are proprietary. In these cases, estimates were based on consultation with OpenHydro. Overall, the dimensions and material properties supplied by OpenHydro were sufficient for the analysis.

2.1.1 Turbine Design and Blade Material Properties

The proposed device for deployment in Admiralty Inlet is an open center OpenHydro tidal turbine with a nominal diameter of 6 m; the diameter of the rotor blades within the duct is 4.8 m. The rotor has a mass of 6,200 kg. Figures 1 and 2 show the spacing between the blade faces. Figures 3 and 4 show the angles between the outer and inner blade edges. The blade has a blunt edge on both edges of the blade.

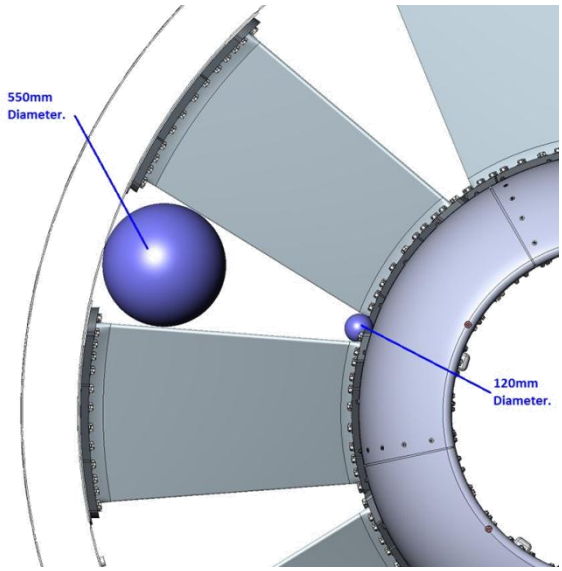

Figure 1. Front view of blade with spacing dimensions of blade edges

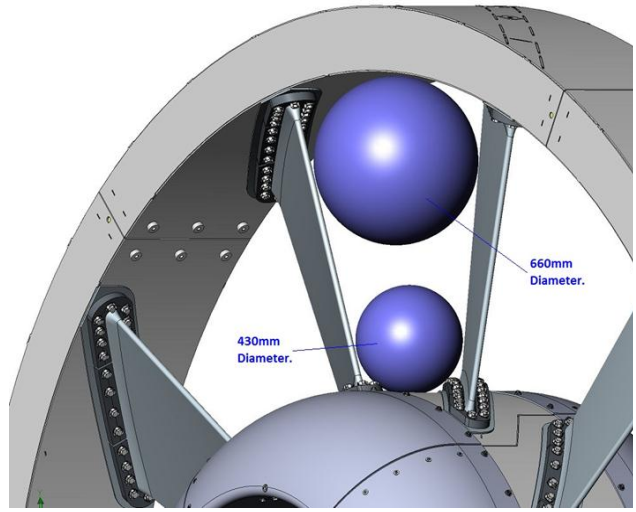

Figure 2. Isometric view with spacing between blade faces

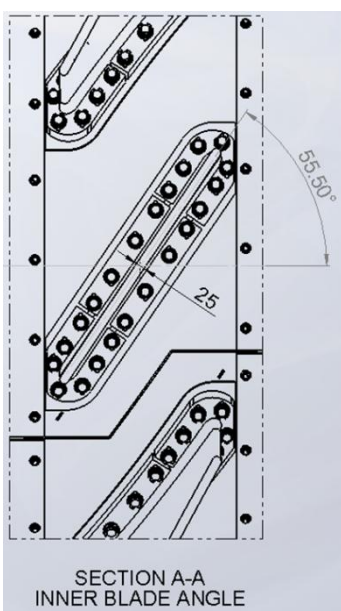

Figure 3. Angles between inner blade edges

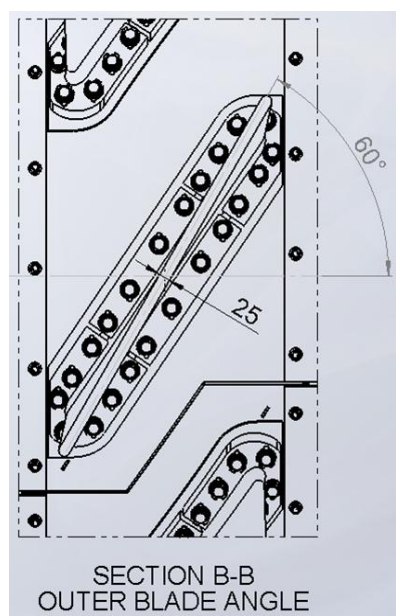

Figure 4. Angles between outer blade edges

Based on communications with OpenHydro, the blade material properties could be adequately estimated using a stiff plastic or composite material. Using either fiberglass composite or plastic resin such as Delrin would be adequate because either is far stiffer than the SRKW material properties. An

elastic modulus (material property defined as stress over strain for elastic deformation under an applied force) of 7 kPa was chosen for the blade based on information provided by OpenHydro.

The moment of inertia for the turbine could be adequately estimated assuming the rotor is a solid disc with a mass of 6,200 kg and diameter of 4.8 m.

2.1.2 Rotor Rotation Rates and Blade Speed

From the information supplied by OpenHydro and the expected tidal velocities within the Admiralty Inlet deployment site supplied by UW–NNMREC, the blade velocities can be calculated anywhere along the radius of the blade edge. Figure 5 shows the probabilities for the maximum possible velocity at the blade tip. Note that this is not an expected impact location for an SRKW. The maximum expected impact scenario is discussed in the following section.

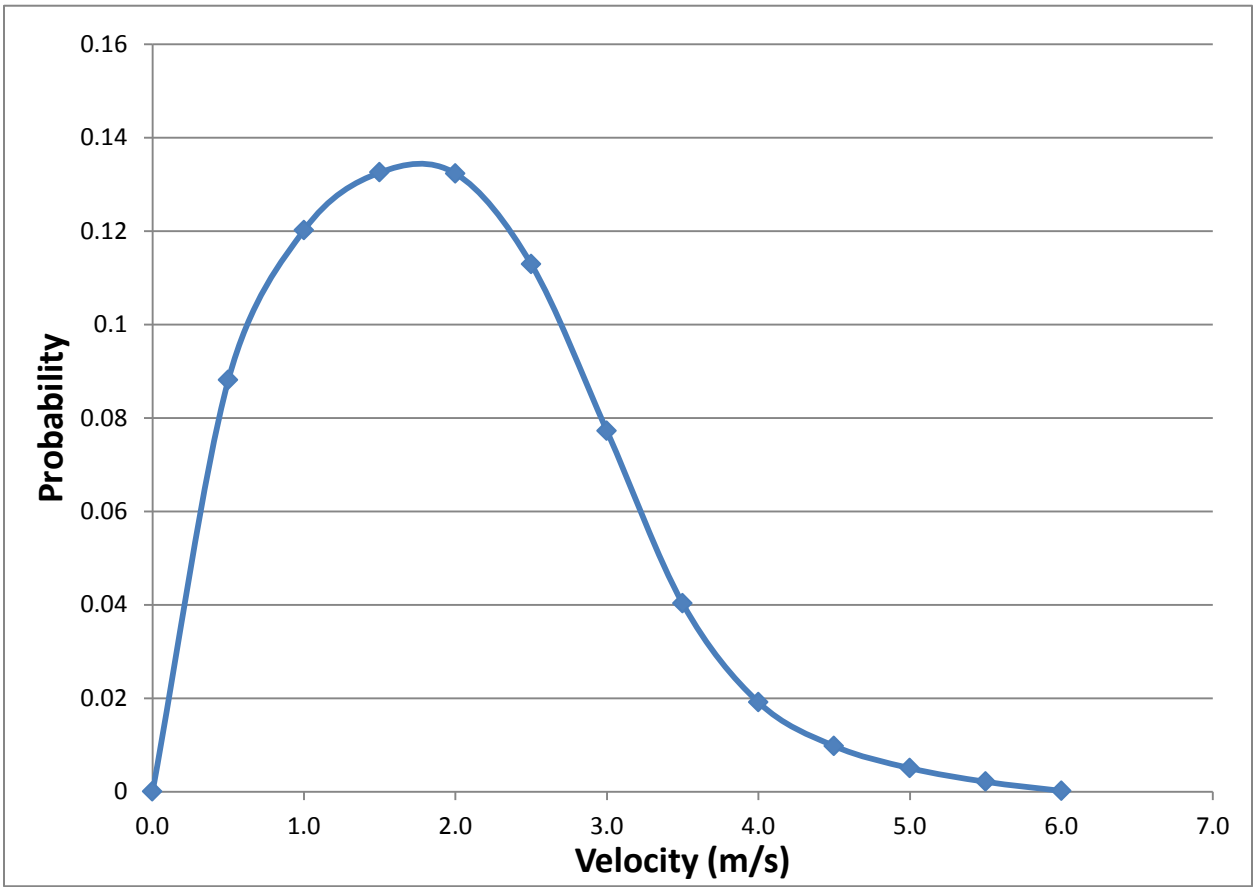

Figure 5. Probability distribution of velocity at blade tip. At low tidal velocity (26% of the time), the blade is stationary (not shown here).

2.2 Blade Impact Scenarios and Physical Characteristics of a SRKW

2.2.1 Blade Impact Scenarios

A recent publication from Durban et al. (2009) contains field data for adult male SRKWs. An adult male was chosen because it has the greatest mass, forcing the affected tissue to absorb a maximum amount of the energy; this will result in little momentum exchange to move the whale mass out of the way of the turbine. The largest adult male reported by Durban et al. was used (Figure 6); the tail section was not simulated in the model. The mass associated with the large adult male SRKW was approximately 4,000 kg; this value was used for model analysis.

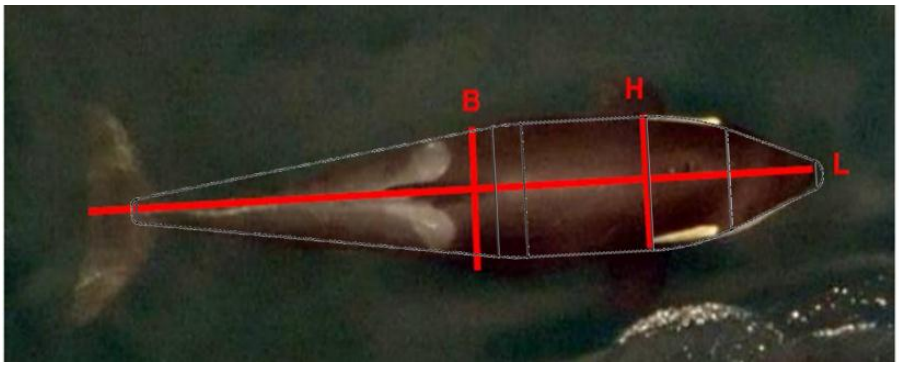

Figure 6. Basic dimensions measured for SRKW (Durban et al. 2009)

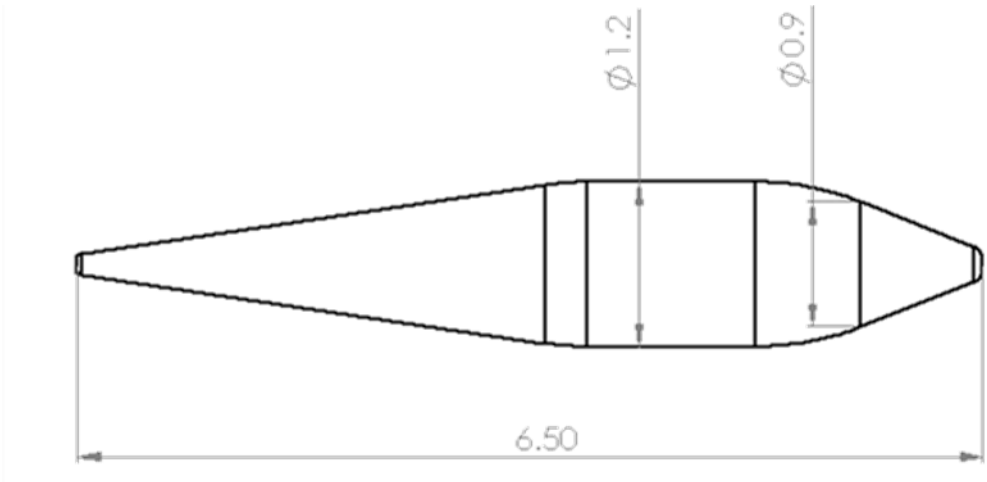

Figure 7. Maximum dimensions reported for an adult male SRKW

It will be difficult, if not impossible, for an adult SRKW to impact the blade at the radius farthest from the center of rotation due to the cowling around the turbine. The most severe impact with respect to tissue damage would be for a large mass (i.e., adult male) to be hit as close to its center of mass as possible. This forces the tissue to absorb more of the impact rather than simply moving the mass (whale) out of the way. If the whales center of mass is far away from the turbine, the turbine force will likely push the mass away; a hit to either end of the whale would likely result in the whale rotating away from

the turbine. It would be unlikely for the whale to become caught in the blades as the blades are angled (Figure 2) and moving slowly (average of 8 RPM). Therefore, the blade velocity used was at the location where the head of the whale could be inserted farthest into the turbine rotor. This causes the most absorption by the tissue due to impact, and the most acute probable injury; thus, this presents the most conservative impact location scenario (Figures 1 and 7). The maximum penetration of the nose of the reference large adult SRKW would extend approximately 0.4 m from the tip of the nose and at a 2.0 m radius on the rotor. In this scenario, the blunt edge of the blade comes in contact with the whale on the top of the head; the eyes are located further back from the place of impact and would not reach into the turbine at the maximum opening between the turbine blades. The probability distribution as a function of blade velocity is demonstrated in Figure 8.

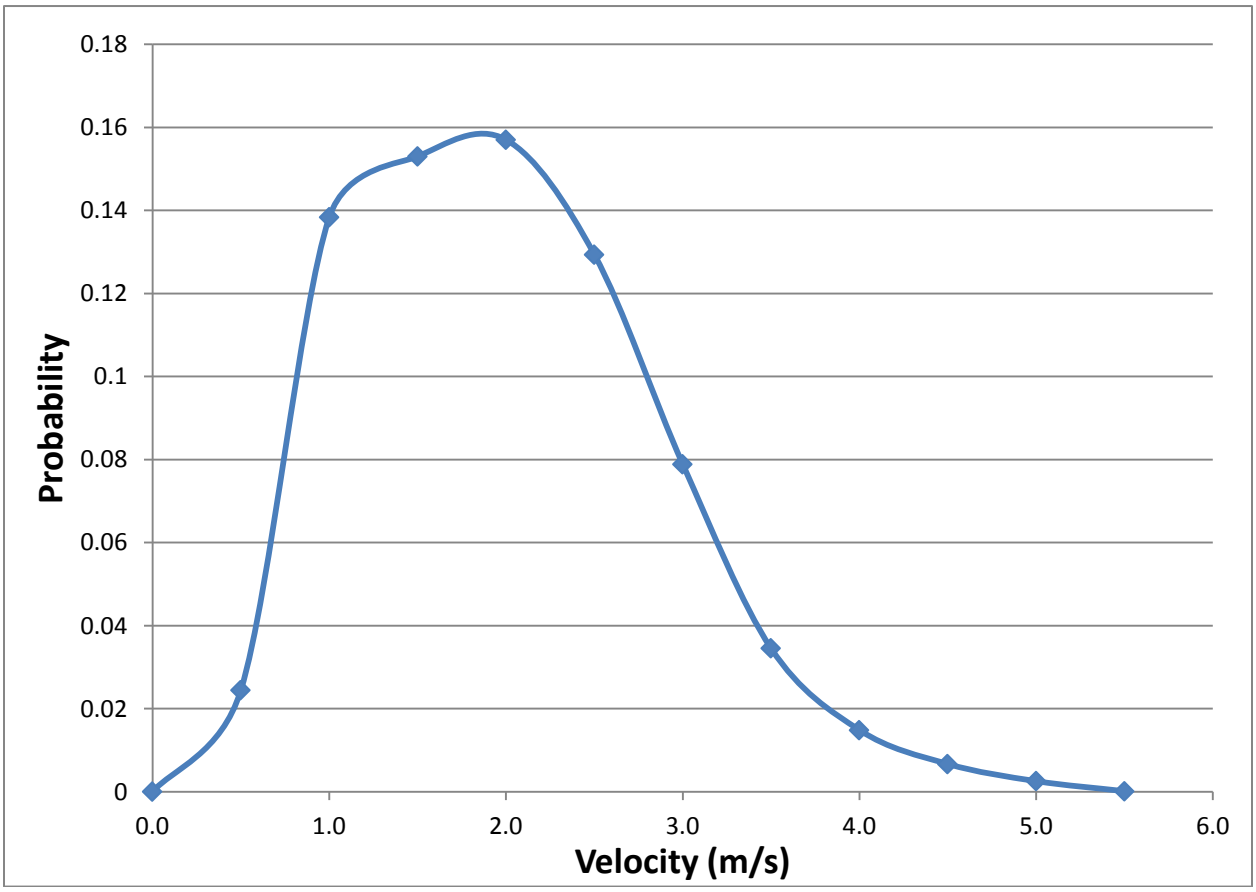

Figure 8. Plot of probability distribution for velocity at a location of 0.4 m from the tip of the blade.

A much smaller juvenile SRKW was also examined with regard to comparative geometry and momentum transfer. In this case, the smaller head of the juvenile SRKW allows for a longer radius of the blade to make impact and impart velocities about 10% higher than what an adult would experience. However, there are more significant issues to address with regard to the momentum transfer and impact force each body experiences. The change in momentum (Δmv) equals the integral of force with respect to time ($\int Fdt$) where impact force and the area the force acts upon is what determines tissue stress. Because a juvenile whale has far less mass (m) than the adult, this lowers the force of the impact and resultant stress significantly compared to a more massive adult. Nevertheless, both the time duration of impact and the impact area will both be smaller for the juvenile which leads to higher tissue stresses for the juvenile

compared to the adult. A simple, closed form impact analysis using colliding blocks of masses (m_{adult} $=8Xm_{juvenile}$) and areas ($A_{adult}=2XA_{juvenile}$) proportional to the adult and juvenile whales demonstrates that the juvenile impact stress would be about 10% less than the adult case. This means that the benefit of a lower juvenile mass is largely negated by the shorter time duration and smaller impact area with regard to material stress. It would be therefore prudent to explore the juvenile case further in subsequent computational models that include the full geometry and material properties for each case.

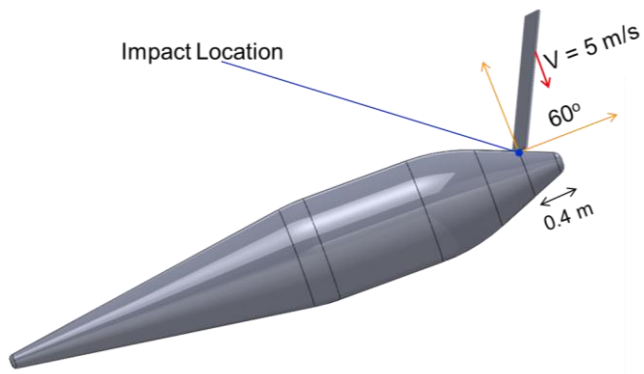

Figure 9. "Maximum velocity" SRKW and blade impact scenario schematic

Other scenarios were roughly considered but have been discounted as they are seen to be too implausible, including

1. a very generalized and conservative closed form solution – This would have a fixed "whale" mass upon impact and include only a single elastic modulus for the whale tissue (blubber).
2. finite element analysis model using blade and whale models from Figure 9 and a variable elastic modulus for whale tissue (blubber) – The whale model will be fixed and thus force the tissue to absorb the impact.

The primary problem with these scenarios is the overly simplistic "fixing" of the SRKW mass. The "fixed" scenario forces the SRKW tissue to absorb all the impact, which is grossly incorrect because the body is, in reality, free to both translate and rotate away from the impact point. The fact that the impact location on the SRKW is a great distance from the center of gravity of the body (~2–3 m) also means that momentum transfer into rotation is significant in this case and should not be excluded from the analysis.

One could also analyze the inclusion of the forward motion of the SRKW by determining the threshold velocity for ramming versus that of curious inspection upon impact with the blade. The blade and forward motion of the SRKW are basically perpendicular, meaning that the resultant velocity vector can be calculated using the Pythagorean theorem. Table 1 shows the resulting blade impact velocity for a range of forward velocities when the blade is moving at 5 m/s.

Table 1. Resultant SRKW impact velocity for 5-m/s blade velocity combined with a range of forward velocities

Forward Velocity (m/s)	Resultant Impact Velocity Vector (m/s)
1	5.1
2	5.4
3	5.8
4	6.4
5	7.1
6	7.8
7	8.6
8	9.4
9	10.3
10	11.2

As the forward velocity starts to significantly (>10% increase) affect the resultant velocity above the maximum blade velocity of 5 m/s, the result approaches ramming scenario (forward velocity > 3 m/s). Previous meetings and discussions have discounted the ramming scenario (in which a SRKW collides with the turbine while swimming at top speed, as in Table 1). The curiosity or "inspection" scenario has the SRKW moving at a forward velocity of 3 m/s or less, as SRKW's typical foraging and traveling speed is about 1.7 m/s (William and Noren 2009: Noren 2011: Baird et al. 2003). The additional computational resources necessary to model both masses (blade and SRKW) moving were not available within the resources of this analysis. Instead, this scenario will be extrapolated from "blade velocity only" simulations. This is a conservative estimate as moving both masses would result in less of the force being absorbed by the whale. Further work will explore the effect of both blade and whale masses moving.

2.2.2 Material Properties for SRKW

Material properties for a Cuvier's beaked whale are available via tissue sample testing and CT scanning from Soldevilla et al. (2005). Table 2 shows the elastic modulus for several tissue types.

Table 2. Elastic moduli (kPa) for several whale tissue types (Soldevilla et al. 2005, Table 4)

	Forehead tissues			Mandible tissues	
Stress (kPa)	Blubber	Acoustic fat	Connective tissue	Blubber	Acoustic fat
2.5	59	75	124	158	78
5	208	153	149	220	215
10	411	212	279	400	303
20	712	412	618	650	420
30	1006	626	1030	913	587
40	1200	739	1295	991	726
50	1410	910	1510	1174	934

These stresses are somewhat lower than what is expected for the impact scenario analysis, and extrapolation may be required to determine the elastic modulus at higher stress states. Figure 10 shows the curve developed by Soldevilla et al. (2005) for stress versus strain of the whale blubber. The data in Figure 10 suggest that the strain and stress for Cuvier's beaked whale tissue reach an asymptote near 1.8

MPa. In addition, the blubber and connective tissue have very similar elastic moduli, and the same value could be reasonably used to represent each. The lower the elastic moduli, the more likely a material is to regain shape after a deformity. Therefore, as a conservative estimate, 1.8 MPa will be used for the elastic modulus of all "non-bone" tissues in the head region.

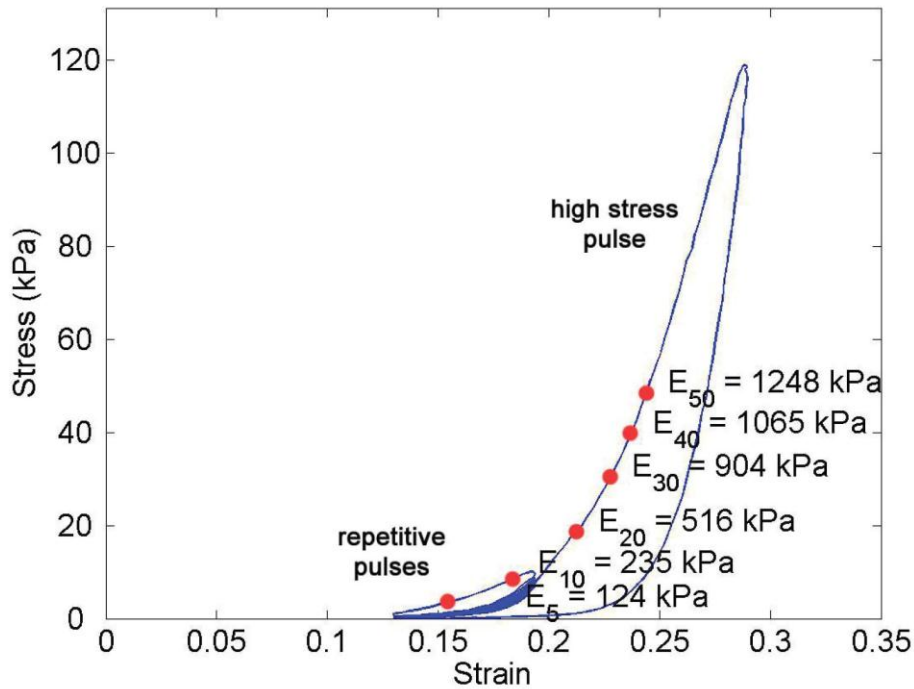

Figure 10. Stress-strain curve for whale blubber (Soldevilla et al. 2005, Figure 7)

Data provided by PNNL for the structure of the head region from McKenna (2005) provide sufficient detail to reconstruct the dimensions of bone matter in the head for use in the model analysis. The material properties of the bone matter can be extracted from Table 4.5 in Campbell-Malone (2007), which provides several values for elastic moduli of right whale (*Eubalaena glacialis*) mandible bone as a function of direction. Although the NARW is much larger than a SRKW and has a more massive mandibular, in the absence of other data, this analysis assumed that the SRKW mandibles have similar biomechanical properties to those of right whales. This assumption is considered to be appropriate as SRKWs are thought to have sturdy mandibles, based on the animals' observed behavior using their rostrums to batter prey animals and battle conspecifics. The average value is approximately 300 MPa for both directional and bone type (trabecular or cortical); this value was used for model analysis.

2.3 Analysis with Finite Element Model

2.3.1 Model Setup

Closed form solutions are available for certain impact scenarios. However, the large deformations and the evolving nature of the contact interface for a blade striking a large mammal suggest the need for a finite element analysis. Figure 11 and Figure 12 show the model domain created for this study. Note that

a symmetry plane is used to reduce the model size. The dimensions are based on a 4,000-kg adult SRKW, as shown in Figure 6. The turbine rotor is represented by a single blunt edge blade (shown in light blue) that is constrained to move in one direction. The ballast elements on the end of the blade (shown in dark blue) are given a very large density so the linear momentum of this massive (4,460-kg) blade corresponds to the angular momentum of the rotor. The skin, blubber, and bone are shown in black, red, and green, respectively. For the engineering analysis, the skin has the same properties as blubber, a conservative approximation since skin would distribute the load from the force of the blade. The model domain does not include the surrounding water that is expected to have a modest effect on the peak loads; this simplification reduces the model size and complexity. Including the surrounding water in the domain necessitates significantly more computational resources than are currently available with the funding and schedule restraints of the project. The average magnitude of the velocity for the moving portion of the whale body upon impact is quite slow and the drag forces in water are $F = \frac{1}{2} A\, C_D\, \rho\, V^2$, with C_D (drag coefficient) being approximately 1 for a cylindrical shape. At peak load for the 3 m/s impact scenario, the only portion of the whale that begins to move is the forward region of the head from the point of impact to the tip of the nose which is about 0.4 m in length. The velocity of this region is about 2 m/s and the area perpendicular to the velocity of the moving portion is about 0.2 m^2. This means the restraining forces by the water on the body during peak loading is a about 400 N or 100 lbf, which is quite small in comparison to the average 4,000 kg of an adult SRKW. Therefore, the surrounding water should not have a large confining effect at these impact speeds.

Table 3 lists the material properties used for the engineering study. All materials are treated as linear elastic because the available material data are limited. The elastic modulus of the blubber is based on the slope of a stress-strain curve (Figure 10) at the maximum value (120 kPa). The Poisson ratio for the nearly incompressible blubber and bone were chosen to match the measured sound speeds. The blubber and bone materials use a Neo-Hookean constitutive model that is valid for large deformations.

More complex material models could be utilized, provided actual test data for the skin and blubber were available. Highly deformable materials such as skin, blubber, and rubber respond differently in tension and compression, and the load-deflection behavior can be very nonlinear. These materials can be represented with a hyperelastic constitutive model such as the Mooney–Rivlin model available in the SNL code, Presto (Koteras et al. 2006). These models have parameters that must be determined by testing specimens under different loading conditions (tension, compression, and shear). The tests are then analyzed with the chosen parameters to ensure the fit adequately represents the measured behavior. Some finite element codes automate the process and accept various types of test data and determine the parameters for the selected constitutive model. However, these essential data are not available for skin, blubber, or rubber; a linear elastic treatment was employed instead.

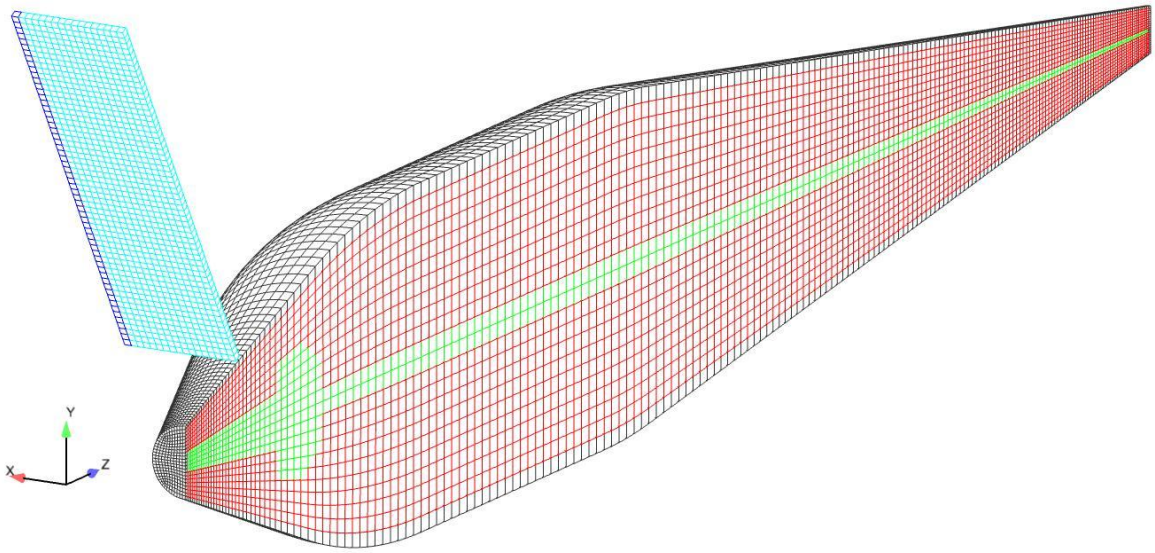

Figure 11. Finite element mesh

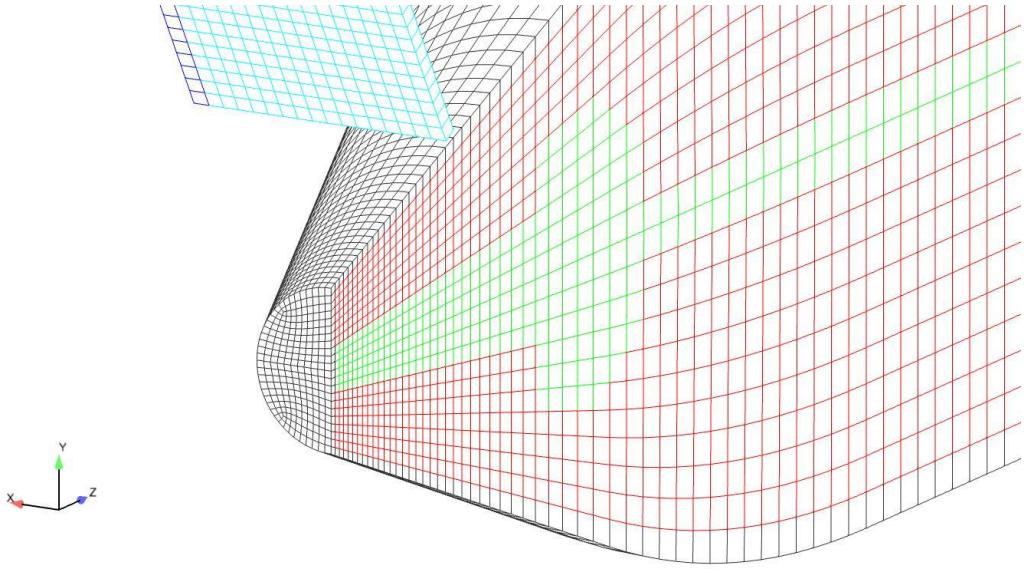

Figure 12. Finite element mesh, impact region

Table 3. Material properties used for analysis

Material	Elastic Modulus (MPa)	Density (kg/m3)	Poisson's Ratio
Blubber[(a)]	1.8	1,000	0.4998
Bone[(a)]	300	1,000	0.4745
Blade	7,000	1,200	0.3
Ballast	7,000	2,325,100	0.3

(a) Blubber and bone constitutive models are valid for large deformations.

2.3.2 Impact Analysis Results

The transient dynamics code Presto was used to consider impact speeds of 1 to 5 m/s. This range is based on the shapes of the MHK device and a SRKW, as well as the expected range of the rotor's angular speeds. In these simulations, the heavy blade is given an initial velocity, and its edges are allowed to translate but not rotate. The blade slows a small amount as it pushes the whale out of the way. Figure 13 shows the force– time histories for several velocity cases. Due to element distortion issues, the simulations with the standard blade could not run to completion for speeds greater than 3 m/s. This is a computational artifact because large shear deformations caused an element nearest the impact to invert but does not imply tissue damage.

Figures 14 through 17 show the strain and pressure contours in the blubber and skin at approximately peak load for two impact velocity cases of 1 and 3 m/s. Table 4 shows the peak stress and strain for each simulation. Although the images in Figures 14 through 17 show what appears to be dramatic depression of the tissue, and the maximum principal (logarithmic) strains might cause tearing in many structural materials (e.g., steel, glass composites), these levels are quite acceptable for materials like human skin, tissue, or natural rubber. For comparison, one could produce similarly proportional depression and strain (with little discomfort) by simply pressing one's index finger into one's thigh. In addition, the computer visualization in Figures 14 through 17 does not definitively represent how the tissue would deform, but instead it computes the resultant stress and forces on the whale.

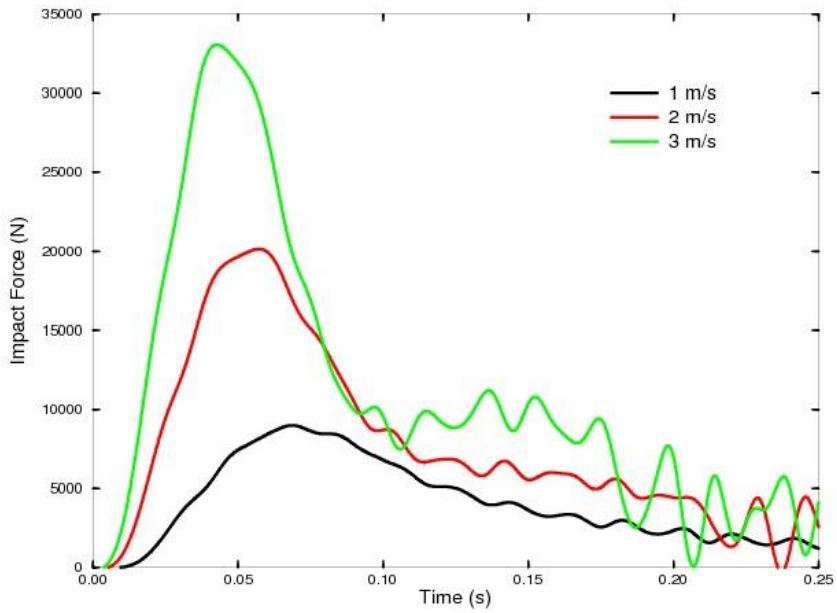

Figure 13. Impact force as a function of time for different blade speeds

Table 4. Peak stress and strain from computational simulations

Blade Speed (m/s)	Blade Type	Maximum Principal Log Strain	Maximum Pressure (kPa)
1	Standard	0.26	950
2	Standard	0.41	1650
3	Standard	0.57	2340
4	Standard	n/a	n/a
5	Standard	n/a	n/a

It should be noted that the peak strains and pressures listed in Table 4 occur in small volumes of tissue and are affected by the element size. Nevertheless, it is reasonable to compare results for different speeds and blade types because the same whale model was used for all of the simulations.

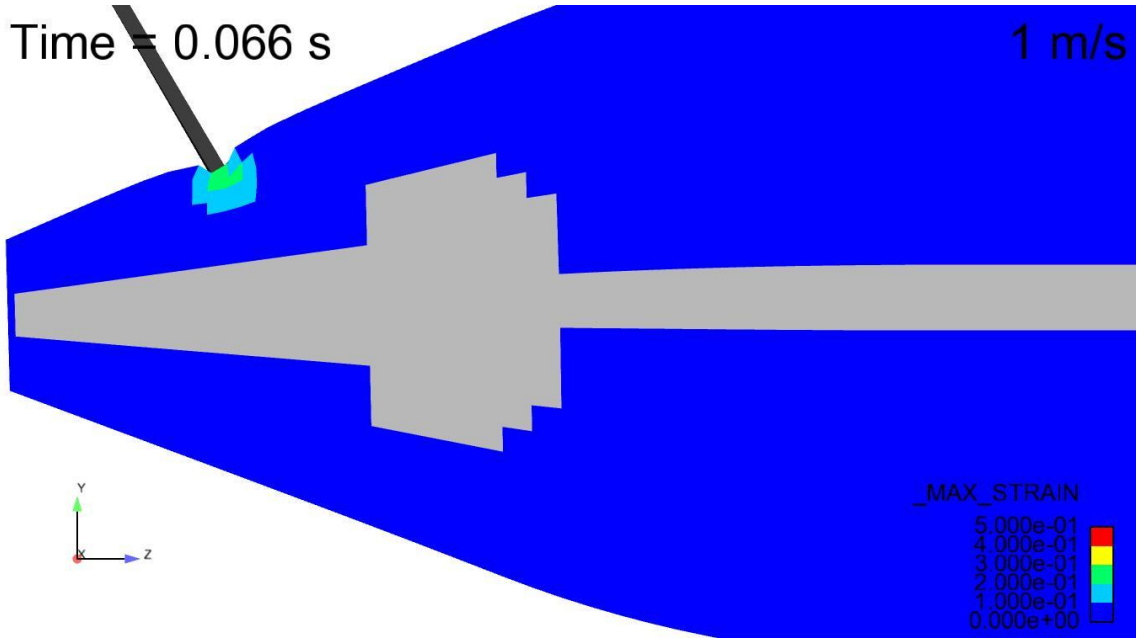

Figure 14. Strain, standard blade, 1 m/s at peak load

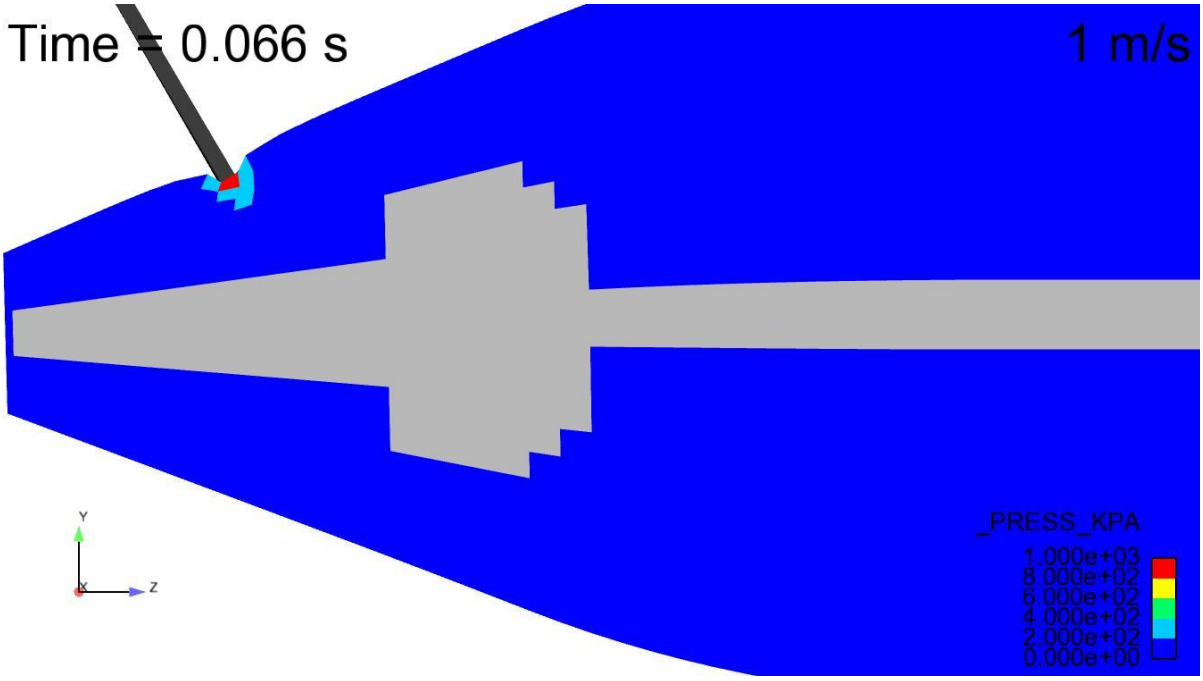

Figure 15. Pressure, standard blade, 1 m/s at peak load

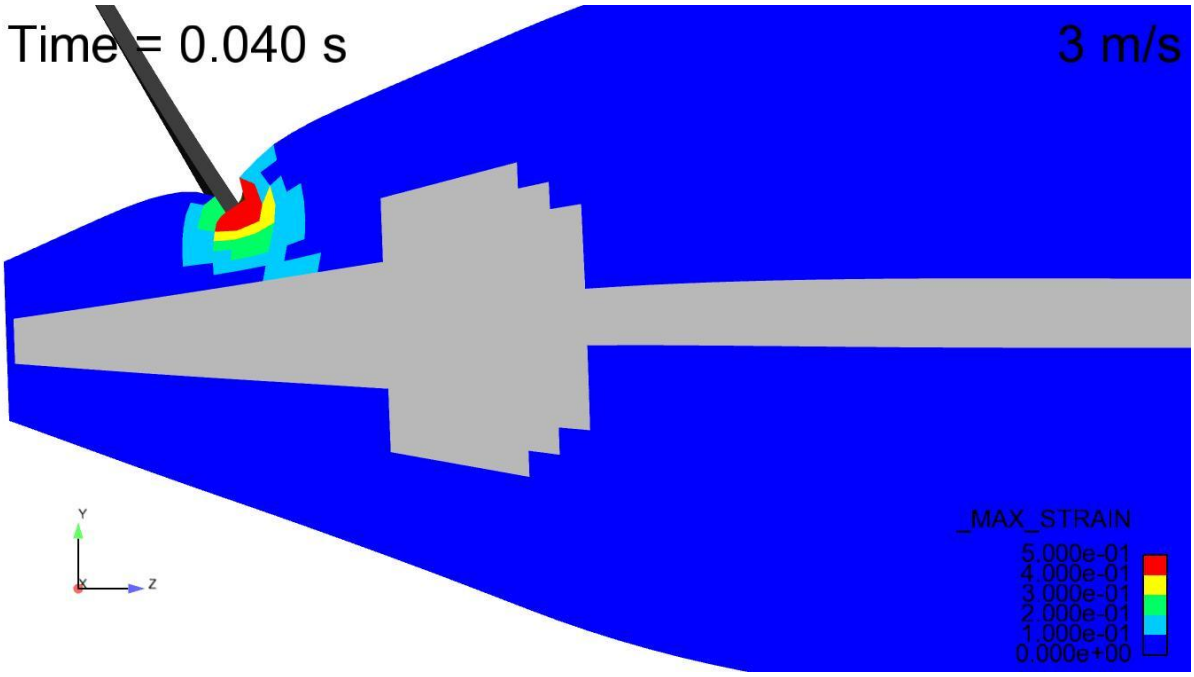

Figure 16. Strain, standard blade, 3 m/s at peak load

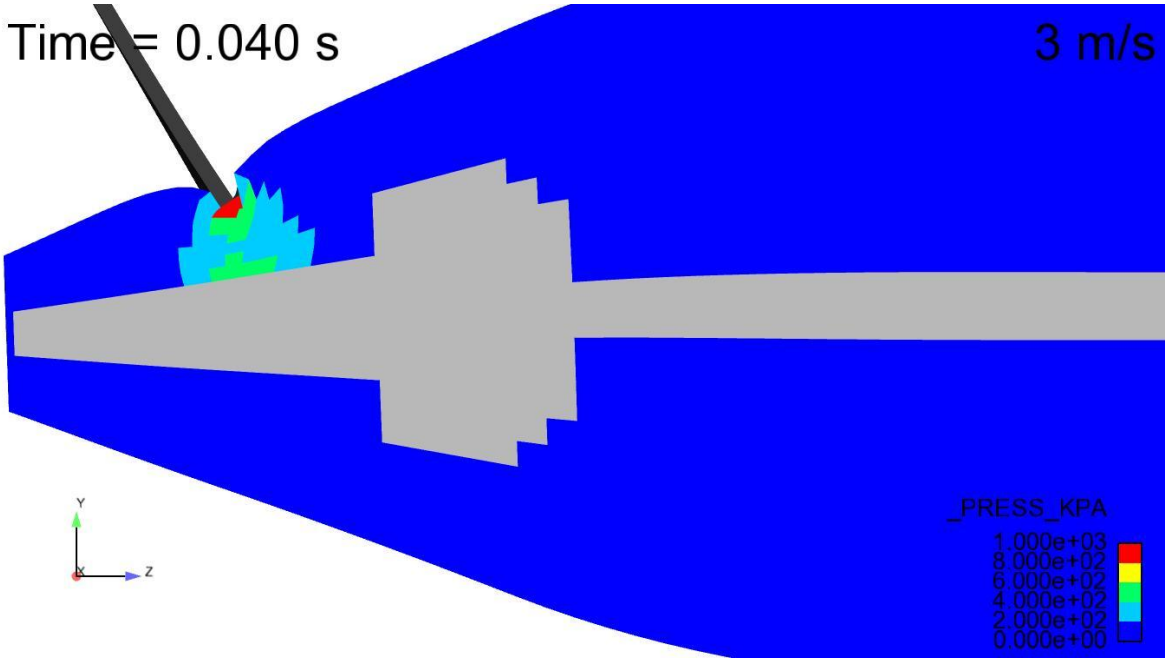

Figure 17. Pressure, standard blade, 3 m/s at peak load

The model simulations could not be computed for impact velocities above 3 m/s due to the computational artifact of element distortion and inversion. However, if it was assumed that the response

was linear between 3 and 5 m/s impacts, one could extend the trend from 1 to 3 m/s simulations to estimate strain and stress at the higher velocities. Figure 18 shows a plot of maximum strain and stress versus impact velocity. The relationship is linear within the velocity ranges at which analyses were completed (1 to 3 m/s) and is indicative of the linear material model used for the tissue. Further analysis could be done to better discretize the model elements and modify time steps to determine if the above assumptions are correct within the range of interest. Based on the linear correlation, the following equations can be used to predict strain and stress for velocities between 1 and 5 m/s:

$$\text{Strain} = 0.1 + 0.15V \tag{1}$$

$$\text{Stress} = 250 + 700V \tag{2}$$

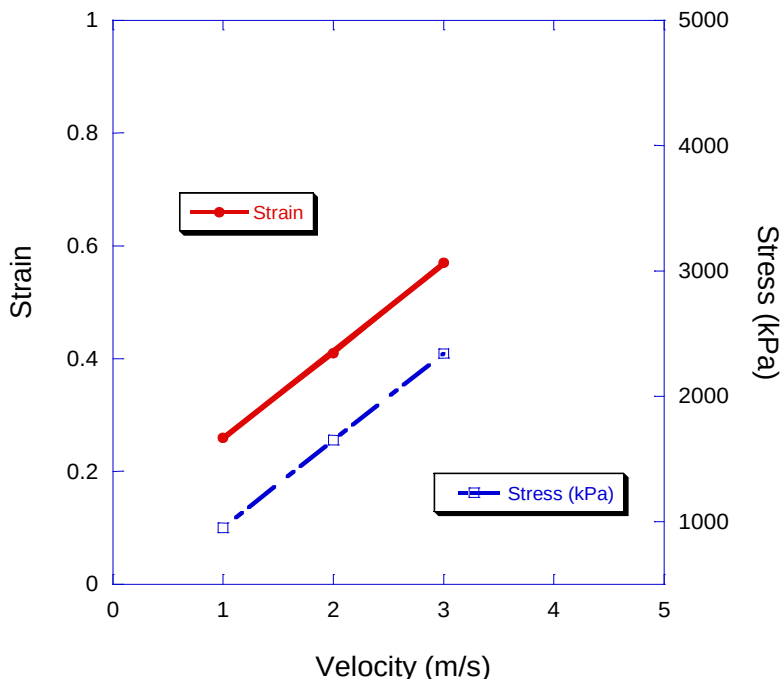

Figure 18. Maximum strain (log strain) and stress versus impact velocity

Table 5 summarizes the peak strain and stress from Equations (1) and (2). These would be reasonable values for determining tissue effects due to impact.

Table 5. Peak stress and strain from Equations (1) and (2)

Blade Speed (m/s)	Maximum Principal Log Strain	Maximum Elongation (%)	Maximum Pressure (kPa)
1	0.25	28	950
2	0.40	49	1650
3	0.55	73	2350
4	0.70	101	3050
5	0.85	134	3750

2.3.3 Including Forward Velocity of SRKW

One could include the contribution of a forward swim velocity of the SRKW by using Equations (1) and (2) and data from Table 1. Results from Noren (2011) for swimming speeds of killer whales under various scenarios suggest that a maximum swimming speed of 3 m/s is reasonable. This would create a net impact of 5.8 m/s if the blade were moving at its maximum speed of 5 m/s. Using Equations (1) and (2), the resulting stress would be 4.310 MPa and the log strain would be 0.97 or 163%. Again, further analysis could be done to both include both the blade and whale bodies moving along with better model element and time step modifications such that convergence is obtained for higher impact velocities. This analysis would provide more realistic non-linearities of the response along with more realistic impact geometries with both bodies moving. This would confirm that the assumptions thus far are correct or the results need to be modified.

The modeling results showed maximum stresses (pressure) for turbine blade strike of the head of an adult male SRKW of about 2.350 MPa, with a strain (tissue elongation) of 73% for the most probable rotation speed of the turbine. Common stresses that can be compared with the stress of a turbine blade encountering a SRKW, as calculated by the engineering analysis include: the stress of a baseball bat hitting a baseball pitched at 90 mph (72.98 MPa); the stress to a player's head from heading a soccer ball moving at 29 mph (.47 MPa). Although there are no publically accessible data that measure the stress of a ship striking a whale, it has been calculated that a 5000 metric ton ship moving 17 mph, where the bow of the ship strikes a .5 inch x 24 inch area of a whale, the stress would be 25.33 MPa, over 10 times the stress forces calculated for the turbine strike.

3.0 Biological Assessment of Consequences of Impact

There is a paucity of data available on the biomechanics of SRKW tissues under compression, particularly skin, creating a challenge for estimating the potential effects of a turbine blade strike. The finite element modeling and engineering analysis carried out by SNL relies on the technical data provided by the turbine manufacturer and physical principles. The SRKW modeled in the finite element model was composed of a single layer of tissue, essentially a whale made entirely of blubber. The choice of this structure introduces a conservative element to the outcome, as the skin of marine mammals (particularly predatory animals such as SRKWs that use their heads to batter prey) is known to be stronger and more resistive to puncture and deformation. In the real world, the forces from a tidal turbine blade strike that might cause injury to the "all blubber" whale will cause less damage to the living animal. The scarcity of biomechanical data for compression deformation and puncture of the SRKW's skin led the PNNL researchers to seek adequate surrogates to estimate the likely outcome of a turbine blade strike. Natural and synthetic rubbers materials were deemed to be most similar (although somewhat more fragile) than SRKW skin. The lack of biomechanical compression measurements did not allow for calculations with which to modify the engineering analysis; rather these assessments of surrogate tissues further reinforced the concept that the assessment of potential harm to the SRKW from a tidal turbine strike is a conservative estimate.

3.1 Whale Head Morphology

The engineering analysis modeled an adult killer whale that was approximately 650 cm in length, not considering the whale's flukes, and weighed 4,000 kg. PNNL was able to locate CT scan data for the head of an adult female that weighed approximately 5,300 kg and was roughly 670 cm in length, including the flukes. Because of the similarity in size to the modeled case, the CT scan data is a reasonable example of the size and location of features in the head of a killer whale of the size modeled in the engineering analysis. The yet unpublished CT scan data presented in this report were made available by Ted Cranford of Quantitative Morphology Consulting, Inc., and are reproduced here with his permission.

Figure 19 shows a sagittal slice through the head of the whale. The location of the transverse slice shown in Figure 20 is located approximately 40 cm from the anterior tip of the whale's head. The intersection of the transverse slice line and the upper surface of the whale's head is the approximate location modeled as the location of impact of the turbine blade on the upper surface of the whale's head.

Figure 20 shows the CT scan for a transverse slice through the head of the whale, as indicated in Figure 19. This slice intersects the lower mandibles of the whale's jaw, which are the "hook"-shaped images to the right and left of center. The hollow voids in the whale's lower mandibles are filled with acoustic fat and other soft tissue and are believed to have a function in the reception of sound by the whale.

The whale's head is approximately 912 mm thick along the transverse slice line shown in Figure 19. In Figure 19, it appears that the mouth of the whale may have been somewhat agape when the head was scanned. However, even considering this condition, it is clear from Figure 19 and Figure 20 that the outline of the whale's head is oblong in shape, being compressed laterally. These images and data were not available when the finite element model of the whale's head used in the engineering analysis was

constructed or when assessment of the extent of exposure of the whale's head to the turbine's blades was made. Given the turbine blade spacing of 550 mm shown in Figure 1, assuming that the approach of the whale would be straight toward the blade assembly, it seems that whales the size of this adult female would most likely not be able to extend their head into the blade assembly (blade length on the order of 1,250 mm) to the extent used in the model, even more so if the turbine's shroud were considered in the analysis. Modeling the location of blade strike further forward on the whale's head makes the assessment of the force of the strike absorbed by tissue conservative because the amount of blade strike energy that would have gone into "pushing" the whale away from the blade is increased as the location of strike is moved away from the center of mass of the whale. However, there is less soft tissue on the anterior of the head, so that a strike in this location might result in more severe consequences. Stranded pilot whales have been noted to sustain the greatest number of injuries on the forward (ventral) third of their heads, however no indication is clear as to the cause of the injuries. Most of the injuries were shown to be non-lethal (Oremland 2010).

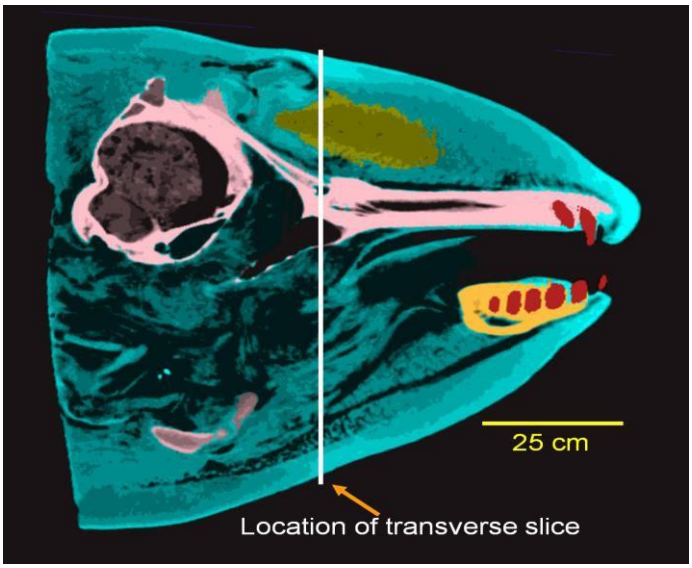

Figure 19. A sagittal CT scan of the head of an adult killer whale. Bone is shown as pink with the lower mandible in orange, teeth as red, voids are black, and other tissues in various other colors. Portions of the upper mandible of the whale's jaw and a cross section through the whale's skull are clear.

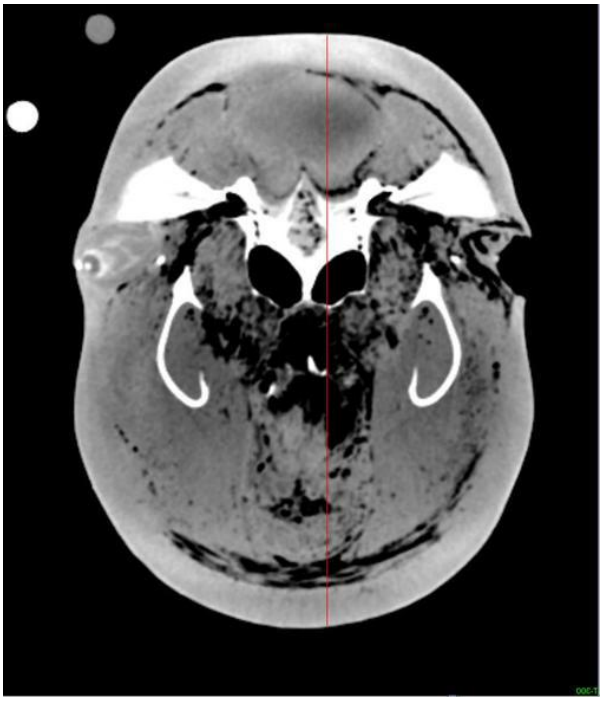

Figure 20. CT scan of a transverse slice through the head of a killer whale approximately 40 cm from the tip of the whale's snout. The red line identifies a transect through the slice where CT scan image intensity values were sampled. In this figure, bone is white, voids are black, and other tissues are gray.

Figure 21 shows the CT scan image intensity data along a vertical transect through the transverse CT scan slice shown in Figure 20. CT scan image intensity data is proportional to the density of the tissue and bone. The *x*-axis is incremented in index units that correspond to a physical length through the head of the whale of approximately 2.5 mm each. The *y*-axis indicates the transmissivity of the tissue to the radiation. In Figure 21, the first data points on the left are for higher-density skin and fibroelastic connective tissues, followed by lower-density adipose and other tissue. Bone has the highest image pixel intensity. These data can be used to estimate the thickness of various tissues and the location of bone relative to the surface of the whale's head. Along this transect, it is estimated that the high-density tissue of the whale's skin and fibroelastic tissue are approximately 50 mm thick, and the lower-density adipose and connective tissue between this layer and the maxilla bones is on the order of 200 mm thick. In total, there is approximately 250 mm (9.8 in.) of tissue with varying density and biomechanical properties between the upper surface of the whale's head and upper mandible bone, along the transect shown in Figure 20. The tissues overlying the mandible in whales probably act as a "bumper" that absorbs and redistributes stresses applied to the surface of the whale (Campbell-Malone 2007).

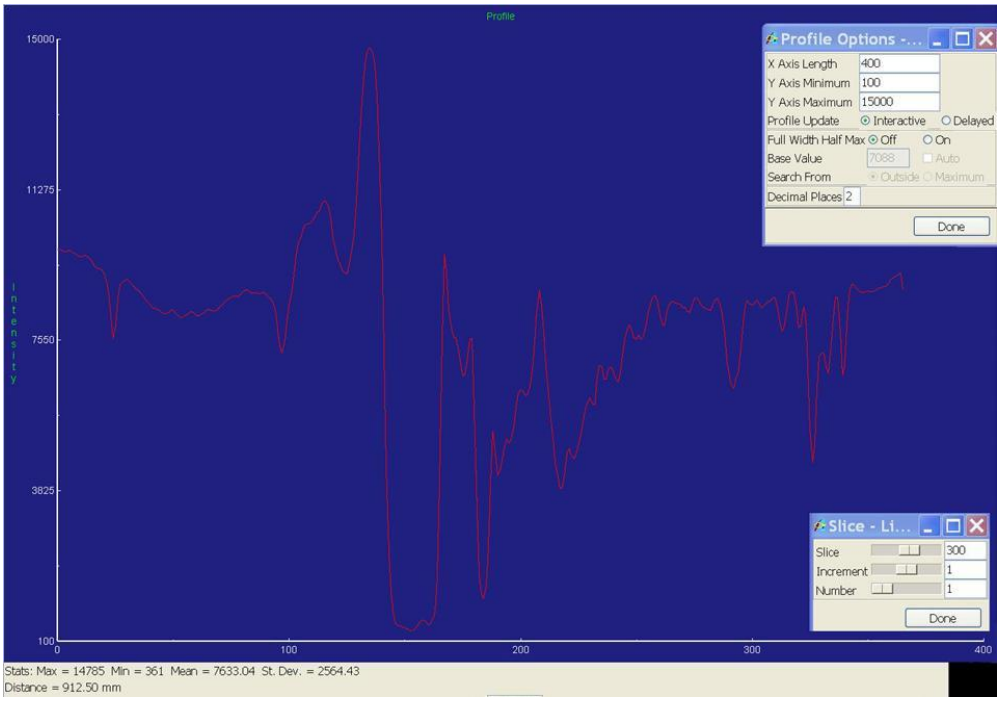

Figure 21. Intensity values along a vertical transect through a transverse slice of CT scan data for the head of a killer whale

The engineering analysis used the biomechanical properties of a single tissue (blubber) to model the SRKW head tissue at and below the location of the blade strike, as there were no biomechanical data for SRKW skin and higher-density fibroelastic tissues at the time of the analysis. However, the CT scan data make it clear that there are multiple layers of differing densities and likely different biomechanical properties. Based on these findings, the forces modeled and potential effects on the SRKW strike by a turbine blade are conservative. By adding biomechanical information on the high-density skin and fibroelastic layer, the force of a blade strike would be distributed over a larger tissue area and would probably result in lower maximum pressures.

3.2 Tissue Models and Biomechanical Data

Review of the published and gray literature, augmented by contact with known marine mammal researchers, determined that there are limited data for the biomechanical properties of whale tissue in general and for killer whales in particular. The majority of biomechanical data available have been taken primarily to investigate the production and reception of sound by those species that use echolocation to communicate and find food. For this reason, there is limited information on the elastic region of tissue and bone stress-strain relationships and few available studies examine other tissue properties such as the stress at which tissue mechanically fails. Hanson studied the failure of harbor porpoise dorsal fin tissue from the stress due to radio tags (Hanson 2001). There is ample biomechanical information over a range of stresses for blubber (Soldevilla et al. 2005) and some information for whale bone (Campbell-Malone 2007). However, there are almost no biomechanical data for whale skin and higher-density fibroelastic tissue.

Because it is known that the skin layer plays an important role in mitigating impacts to the surface of all animals including whales, an effort was made to examine available information and to identify a material with known properties that might be used as a surrogate for whale skin. We performed a literature review to determine if mechanical properties could be identified or inferred for killer whale skin.

The modulus of toughness is an important stress-strain feature of a material (such as whale skin) and is characterized by its ability to absorb energy. The modulus of toughness is equal to the area under the stress-strain curve from the origin through the ultimate yield or rupture point for the material. As the term implies, toughness refers to the ability of a material to absorb energy without breaking. Unlike the modulus of elasticity, which is the constant of proportionality between stress and strain for elastic materials that respond linearly to stress, the "modulus of toughness," U_T, is a characteristic associated with susceptibility to puncture and laceration damage from mechanical trauma. The modulus of toughness is defined as the measure of a material's ability to plastically deform without fracturing. This is represented graphically in Figure 22. It is related to impact strength through the following equation:

$$U_t = 1/3(\varepsilon_{Br})(\sigma_{yp} + 2\sigma_{ult}) \quad (3)$$

The literature review determined that very little information exists for mechanical properties of whale skin. J.P. Winn (2006), in a master's of science thesis that investigated the physical response of whale tissue to entanglement, reported that

> The dermal layer is composed of an extensively cross-linked network of collagen fibers that may function as an elastic recoil mechanism during swimming activities. However, to date the only structural studies on cetacean epidermis have been measurements of epidermal thickness and evaluations of surface properties, including surface roughness and resistance to biofouling. Epidermal thickness … ranging from a minimum of 1.4 mm to a maximum of 25 mm in fin (*Balaenoptera physalus*) and bowhead whales (*Balaena mysticetus)* respectively.

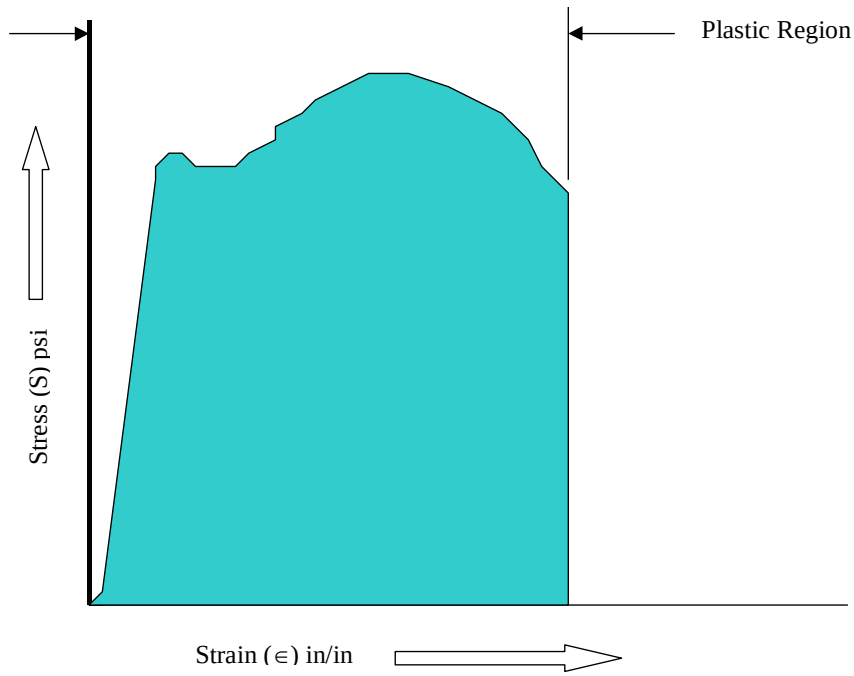

Figure 22. Description of material toughness in the context of stress-strain dynamics

Table 6. Comparative epidermal ranges reported for baleen whale species (Winn 2006, Table 1)

Epidermis Thickness:								
Species	Gender	Length (cm)	Maximum Thickness (mm)	Source	Gender	Length (cm)	Minimum Thickness (mm)	Source
Balaena mysticetus	-	-	25.0	Haldiman *et al.* 1985	-	-	8.6	Haldiman *et al.* 1985
Balaenoptera acutorostrata	-	-	3.0	Singarajah 1984	-	-	3.0	Singarajah 1984
Balaenoptera acutorostrata	F	708	3.0	Sokolov 1982	F	708	1.4	Sokolov 1982
Balaenoptera physalus	M	1565	3.9	Sokolov 1982	F	1600	2.5	Giacometti 1967
Eubalaena glacialis	M	1075	13.2	Sokolov 1982	F	1630	8.6	Sokolov 1982
Megaptera novaeangliae	M	857	5.6	Jones and Pfeiffer 1994	M	857	4.3	Jones and Pfeiffer 1994

Winn's thesis contains results from abrasion tests on whale epidermis using 6.4-mm and 9.5-mm float line. Tests used straight pull and oscillatory pull under load to evaluate the effects of movement of rope across whale skin. The intent of the experiments was to model injury to the skin of whales struggling to free themselves from entanglement.

Observations from both bowhead and right whales indicate that the primary strength in the epidermis is oriented in a vertical direction while laterally the structure is more

elastic with lower strength. From a structural standpoint, this type of fiber integration would have several mechanical advantages. Strong vertically oriented fibers would both increase the abrasion resistance of the epidermis and may help to decrease the compressibility of the layer (Figure 23). As a lateral abrading force is applied to the surface of the epidermis, the strong vertical fibers would start to bend, orienting in the direction of the applied load. This flexure would allow the load to be applied in line with the vertical fibers that are anchored through the entire epidermal layer. Retaining elastic elements between these vertical fibers would maintain the flexibility needed in the epidermis allowing the epidermis to stretch during normal swimming activities. This elasticity may be graded through the stratum intermedium as the degree of keratinization and flattening of the epidermal cells has been noted to increase with distance from the sratum germinativum.

Winn also reports that

The depth of penetration and character of the dermal papillae may also substantially influence the strength of the epidermis as a unit. Assuming that a more multidirectional orientation of collagen fibers in the dermal material enhances the tensile properties of the dermis, the volume of this dermal material interwoven within the epidermis would substantially influence the structural characteristics of the layer.

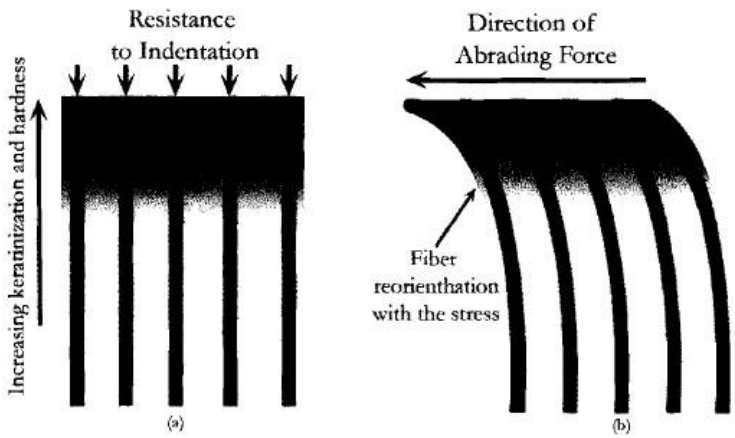

Figure 23. Structural advantages of a vertical fiber orientation within the epidermis. Fibers provide resistance to: (a) indentation and (b) lateral abrasion. (Winn 2006)

Based on the information from Winn (2006), in the absence of biomechanical data for whale skin, hyperelastic material was used to examine the SRKW skin layer in our post-engineering analysis. Figure 24 and Table show properties of rubber and various elastomers.

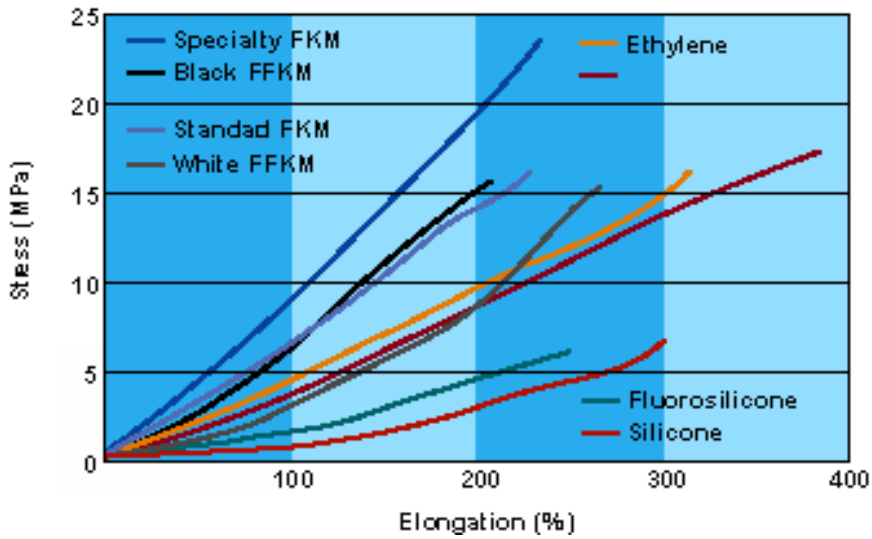

Figure 24. Examples of stress-strain characteristics for some manmade elastomers (*The Physics of Rubber*, http://www.allsealsinc.com/allseals/Orings/or13.htm)

Table 7. Properties of various elastomers (Schaefer 2009, Table 33.2)

ASTM designation	NR	BR	SBR	IIR CIIR	EPM EPDM	CSM	CR	NBR	HNBR	ACM ANM	T	FKM	FVMQ	VMQ MQ, PMQ, PVMQ	AU EU	GPO	CO ECO
Durometer range	30–90	40–90	40–80	40–90	40–90	45–100	30–95	40–95	35–95	40–90	40–85	60–90	40–80	30–90	35–100	40–90	40–90
Tensile max, psi	4500	3000	3500	3000	2500	4000	4000	4000	4500	2500	1500	3000	1500	1500	5000	3000	2500
Elongation max., %	650	650	600	850	600	500	600	650	650	450	450	300	400	900	750	600	350
Compression set	A	B	B	B	B-A	C-B	B	B	B-A	B	D	B-A	C-B	B-A	D	B-A	B-A
Creep	A	B	B	B	C-B	C	B	B	B	C	D	B	B	C-A	C-A	B	B
Resilience	High	High	Med.	Low	Med.	Low	High	Med.-Low	Med.	Med.	Low	Low	Low	High-Low	High-Low	High	Med.-Low
Abrasion resistance	A	A	A	C	B	A	A	A	A	C-B	D	B	D	B	A	B	C-B
Tear resistance	A	B	C	B	C	B	B	B	B	D-C	D	B	D	C-B	A	A	C-A
Heat aging at 212°F	C-B	C	B	A	B-A	B-A	B	B	A	A	C-B	A	A	A	B	B-A	B-A
T_g, °C	–73	–102	–62	–73	–65	–17	–43	–26	–32	–24, –54	–59	–23	–69	–127, –86	–23, –34	–67	–25, –46
Weather resistance	D-B	D	D	A	A	A	B	D	A	A	B	A	A	A	A	A	B
Oxidation resistance	B	B	C	A	A	A	A	B	A	A	B	A	A	A	B	B	B
Ozone resistance	NR-C	NR	NR	A	A	A	A	C	A	B	A	A	A	A	A	A	A
Solvent resistance																	
Water	A	A	B-A	A	A	B	B	B-A	A	D	B	A	A	A	C-B	C-B	B
Ketones	B	B	B	A	B-A	B	C	D	D	D	A	NR	D	B-C	D	C-D	C-D
Chlorohydrocarbons	NR	NR	NR	NR	NR	D	D	C	C	B	C-A	A	B-A	NR	C-B	A-D	A-B
Kerosene	NR	NR	NR	NR	NR	B	B	A	A	A	A	A	A	D-C	B	A-C	A
Benzol	NR	NR	NR	NR	NR	C-D	C-D	B	B	C-B	C-B	A	B-A	NR	C-B	NR	B-A
Alcohols	B-A	B	B	B-A	B-A	A	A	C-B	C-B	D	B	C-A	C-B	C-B	B	C	A
Water glycol	B-A	B-A	B	B-A	A	B	B	B	A	C-B	A	A	A	A	C-B	B	C
Lubricating oils	NR	NR	NR	NR	NR	A-B	B-C	A	A	A	A	A	A	B-C	A-B	D	A

A = excellent, B = good, C = fair, D = use with caution, NR = not recommended

SOURCE: *Seals Eastern, Inc.*

Table shows mechanical properties from Matbase and Matweb for a wide variety of elastomers. To understand the effects of the whale skin layer from turbine blade impact, it would be advantageous to run multiple engineering models with hyperelastic materials. Materials such as natural rubber and fluorosilicone rubber fall into this category and have properties that bound those of the materials in this category.

Table 8. Mechanical properties of various elastomers (http://www.matbase.com and http://www.matweb.com/)

Material	Ultimate Yield Stress (kPa)	Elongation/Strain %	Young's Modulus (MPa)
Butadiene Rubber	15000	200–400	
Chloroprene Rubber (CR)	25000	100–400	
Chlorosulph PE	20000	200–500	2–15
Ethenepropenediene Rubber	20000	250–500	2–10
Liquid Silicon Rubber	7000	250–550	—
Natural Rubber (NR)	30000	750–850	1–5
Nitrile Rubber (NBR)	20000	200–500	2–5
Silicon Rubber (SI, Q, VMQ)	8000	200–800	1–5
Styrenebutadiene Rubber (SBR)	25000	250–700	2–10
Urethane Rubber	30000	300–400	2–10
Butyl Rubber (IIR, CIIR, BIIR)	17000	400–800	—
Chlorosolfonated Polyethylene Rubber	21000	200–500	—
Epiclorohydrin Rubber (CO, ECO)	17000	150–500	—
Ethylene Propylene Rubber (EPM, EPDM)	17000	600	—
Fluorosilicone Rubber (FMQ, FVMQ, FSI)	8600	100–400	—
Hydrogenated Nitrile Rubber (HNBR)	30000	100–400	—
Natural Rubber, Not Vulcanized (NR, IR,	27600	500	—
Natural Rubber, Vulcanized (NR, IR,	28000	100–800	—
Polybutadiene Rubber (BR)	17000	300–800	—
Polychloroprene Rubber (CR)	28000	100–800	—
Polynorbornene Rubber (PNR)	24000	—	—
Polyphosphazene Rubber (PZ, FZ)	14000	—	—
Propylene Oxide Rubber (GPO)	17000	—	—

3.3 Biomechanics of Human Skin

Human skin has the same basic construction as SRKW skin, with an epidermis, dermis, hypodermis, and a fourth layer connecting the skin to underlying tissue. Human skin has been found to behave as a nonhomogeneous, anisotropic, nonlinear viscoelastic material (Hendriks 2001). A basic function of the skin is to protect the body from mechanical injury.

The stress-strain relationship for human skin is shown in Figure 25. The top line in Figure 25 is the true stress-strain curve for human skin; the two below are elastic and viscous stress-strain curves.

The relationship between stress and strain for human skin shows trends that are similar to those predicted for whale blubber in the engineering analysis performed here (Table 5). The engineering

analysis did not include the epidermis and dermis layers that give skin many of its composite biomechanical properties. The engineering analysis estimated that at a pressure of 2.35 MPa, a turbine speed of 3 m/s would elongate the blubber by about 73%. In Figure 25, it can be seen that this same level of stress experienced by human skin would result in an elongation (strain) of about 60%. At the highest turbine speed for which the response of blubber is considered in the engineering analysis (5 m/s), an elongation of 134% was predicted at a pressure of 3.75 MPa. In Figure 25, it can be seen that for human skin, this level of stress would result in only a small increase in elongation from a stress of 2.35 MPa. The different results between the elongation of blubber and whale skin is probably due to the more viscous nature of blubber and the lower level of elasticity of whale skin. In fact, it is likely that whale skin, because of the differences in the dermal layer between humans and whales, might have a stress-strain curve that would have a steeper slope than that shown for human skin. Stress-strain curves for a harbor porpoise, although tested at much lower forces, appear to support this conclusion (Hanson 2001).

It seems highly likely that consideration of the epidermal and dermal layers of whale skin, in addition to the hypodermis (blubber), would result in values for strain lower than those predicted for blubber alone and at lower stress levels than are likely to damage SRKW skin within the elastic region.

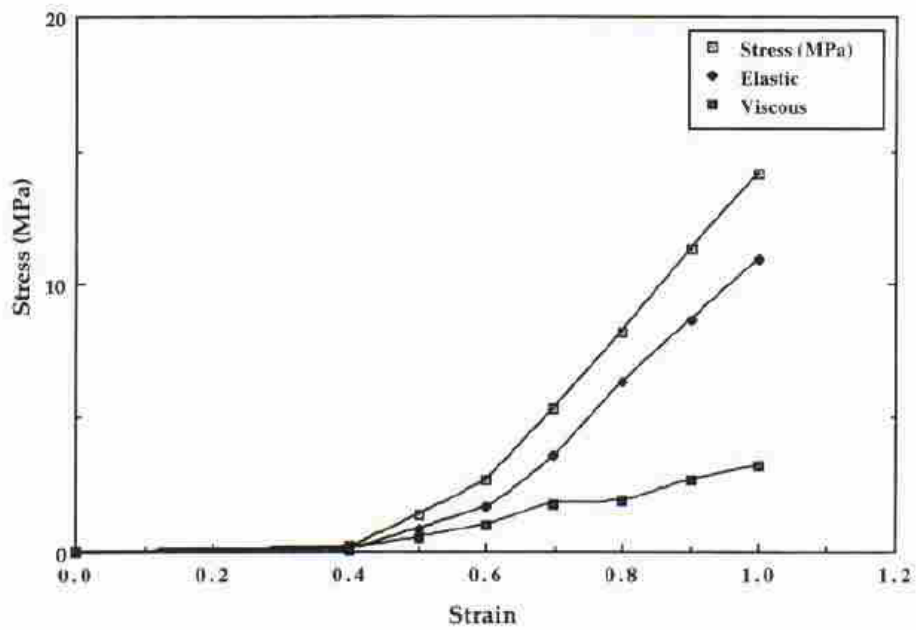

Figure 25. Relationship between stress and strain for human skin showing true stress (unfilled squares), elastic (diamond symbols), and viscous (filled squares) components (after Silver et al. 2001, Figure 2)

3.4 Consequence of Turbine Blade Impact on Whale Tissue

The consequence of tidal turbine blade impact on whale tissue can be roughly estimated from the model data in Table 4. The data in Table 4 are worst case for the soft tissue found below the skin and fibroelastic layers of whale tissue: if included, the skin and associated fibrous layer would have acted as a membrane and distributed the force of the blade strike over a larger area of underlying tissue.

If it can be assumed that whale skin behaves similarly to human skin, the stress-strain curves in Figure 18indicate that at the maximum pressure of 3.75 MPa (3750 kPa), the corresponding strain of 0.73 would remain in the elastic range as shown in Figure 25. Elongation percentages at the highest turbine blade speed would vary between approximately 25% to 200%; the elongation percentage for materials in the middle of the range would be about 100%. At all other blade speeds, elongation would be less. Because the response of these materials is elastic over the range of pressures in Table 4, it is expected that if whale skin behaves similarly to these materials, whale skin tissue would deform at strike and, in conjunction with underlying soft tissue, absorb the force of the strike and would return to normal condition a short time after the pressure was removed. These data indicate that the skin would not fail (i.e., be torn by the impact) at even the highest exposure pressures.

The analysis of the blubber mechanical property data conducted during model construction based on measured biomechanical properties of blubber suggests that blubber has properties that are similar to rubber as well. As such, the whale blubber would display elastic properties with elongation response to stress without deformation within the range of pressures predicted by the engineering analysis. It is possible that within this range of pressure and resulting deformation, the tissues experiencing the highest pressures would bruise. It is expected that the pressures listed in Table 4 would not be realized because the skin and underlying fibrous fatty tissue would deform to distribute the force of the strike across a greater area of tissue.

Campbell-Malone (2007) gives a value for the ultimate compressive strength for trabecular right whale mandible bone of 17.95 MPa. The ultimate strength for bone of the skull would be higher. If this value can be used for killer whale mandibular bone, the highest pressure predicted (3.75 MPa) is well below the pressure at which this bone would be expected to fracture. Because the skin and other tissues overlying the killer whale mandible would absorb most if not all of the pressure from the blade strike, the pressure on the whale's mandible would likely be an order of magnitude or so below a pressure expected to cause fracture.

4.0 Additional Information to Inform Strike Modeling: Blunt Force Trauma and Real-World Experience

Without real world testing for the unique situation of a SRKW impacting a turbine, PNNL researchers aimed to contextualize and verify their results through research into blunt force trauma and consulting marine veterinarians. This additional information aided in understanding the kinds of forces that might injure a SRKW and the resultant potential consequences or behavioral changes.

4.1 Blunt Force Trauma Research

Additional information on potential effects of a turbine blade strike to a SRKW from a blade strike can be gleaned from research and monitoring results of animal head trauma. PNNL researchers searched peer reviewed and gray literature on blunt force traumas of marine and terrestrial mammals. Peer reviewed literature was accessed using Web of Science and gray literature accessed from Google searches and cited references in papers identified from the Web of Science searches. A key index for evaluating the severity of head trauma in humans and other animals has been developed, known as head injury criteria (HIC). Although such an index is not available for marine mammals, the process of developing a HIC might be instructive. While searching for pertinent literature on blunt force trauma, PNNL researchers looked for papers that might support the development of a marine mammal HIC or other types of risk assessment tools for interactions with objects. Literature on large and small terrestrial mammals was also reviewed. This literature review supports some insights into blunt force head trauma in a variety of mammal species and also sheds light on tools and methods that may be useful in assessing and modeling head trauma on SRKWs and other marine mammals.

Initial literature searches were focused on marine mammal and whale head trauma, with most results describing consequences of collisions between ships and marine mammals and also for underwater detonations. However, few studies incorporate information on the forces that caused the trauma, which prevents direct comparison beyond the specific event or collision incident, and provides limited insight into the tidal blade strike scenario. One notable exception is the work by Tsukrov et al. (2009); this study developed a three-dimensional finite element mesh model to predict the mechanical behavior of a right whale's mandibular bone under strain, combined with the potential forces exerted by a whale–ship collision. This information provides insight into how a similar approach could be used to develop mechanical models of the SRKW skull and brain. If these biomechanical models were combined with biological models of brain trauma, the result might inform the potential effects of blade strike on the head of a SRKW.

By widening the scope of the literature search to other animal studies and studies related to traumatic brain injury and HIC development, it became apparent that the animal research community segregates head trauma into three main categories: clinical (research directly involving human subjects), large animal studies, and small animal studies. Literature focused on larger animals showed that porcine studies are most valuable, providing detailed descriptions of brain trauma in pigs after controlled, laboratory-induced head injury, from the sub-cellular to the whole brain level of biological organization. Literature on equine and canine head trauma is more limited; quantitative results on other livestock were not found.

The literature reflects a trend toward increasing reliance on small-animal models for head trauma research, which offer advantages associated with cost, animal welfare/ethical concerns, well-defined protocols for inducing head injury, and more sophisticated analytical tools. Most of the small-animal models are for rodents. The increasing use of rodent model systems for studying traumatic brain injury also coincides with the use of in vitro systems, including isolated brain tissue slices and axonal cell cultures, allowing for better characterization of the cellular mechanisms of injury. The results of the PNNL literature search are available online through the Tethys database (http://mhk.pnnl.gov/wiki/index.php/Orca_Strike_Analysis).

4.2 Assessments from Marine Veterinarians

In the absence of field observations to validate the outcome of the strike analysis, PNNL researchers sought input from marine veterinarians familiar with the effects of head trauma and other injuries in cetaceans and other marine mammals. The veterinarians provided professional insights into effects on marine mammals recovered from strandings and from observations of animals in captivity. In almost all cases, the insight gained from the veterinarians consisted of their best professional judgment and was described through anecdotes rather than through the presentation of data and drawing of conclusions.

Investigations in strandings of marine mammals often do not yield clear cause of death. For example, a young SRKW (L112) was found dead off the coast of Washington State in February 2012. The necropsy outcome[1] reported that the animal

"…showed extensive bruising and swelling on both sides of the head and neck, more pronounced on the right, and continuing down the right side of the body. Although no skull fractures were seen during examination of the head, there was fragmentation of the brain and increased fluid in the right side of the skull. The grossly noted hemorrhage around the head and neck is consistent with physical trauma, which would have been sufficiently severe to account for the loss of this animal. The cause of this injury remains undetermined and investigations are ongoing….".

The marine veterinarians were asked the questions listed below. However, as most of the veterinarians had little to no experience with orca injuries of the type hypothesized by a tidal turbine blade strike, most interviews became free form, with the marine veterinarians offering anecdotes about their experience examining stranded animals and/or caring for animals in captivity. In some cases, the marine veterinarians were able to suggest appropriate papers or reports that offer insight into the potential risk to collisions of marine mammals with other animals or with underwater objects. Their observations pertinent to our study are summarized in the following paragraphs.

- What would you estimate to be the likely outcome of a small whales (orca) swimming rostrum first into a tidal turbine blade, with the blade striking in the head region?
- Do you have any information on the compression biomechanics of orca tissue, particularly the skin?
- Have you experienced, treated, or handled cetaceans that have suffered from blunt force trauma? If so, what objects were responsible for the damage?
- If you have experience with a whale that has been struck, what was the outcome for the whale, particularly in terms of tissue damage (epidermis, dermis, bone, underlying

[1] Southern Resident Killer Whale L112 Stranding Progress Report, May 15, 2012.

hematoma, hemorrhaging, etc.)? How far did the damage spread laterally?

- How long did injuries take to heal?
- How frequently have you seen strike injuries to the rostrum region?
- If you have cared for animals (in captivity) that have struck, were there lasting effects of the strike injury? If so, what were the effects and how long did they persist?

When marine mammals are struck, it is not uncommon to see bruising in the underlying tissue, even if the skin is not broken. The veterinarians look at pink discoloration in the blubber layer as a focal point to investigate for underlying damage, including bone fracture.

Evidence on the effects of propeller strike on smaller marine mammals is most commonly studied in manatees. The dermal layers are thick in manatees as compared to most cetaceans. Mortality in manatees from boat strike is generally due to the combined effects of lacerations and blunt force trauma to the skeleton, including the skull. However, manatees have very powerful bone regenerative capabilities (Dr. W. McLellan, University of North Carolina–Wilmington, personal communication, September 2012). Key literature sources include Kipps and McLellan (2002), Lightsey et al. (2006), and Rommel et al. (2007).

Other marine mammal evidence of interest includes infanticide of harbor porpoise calves caused by attacks from bottlenose dolphins. Porpoise calves (as well as some bottlenose dolphin calves) have died from head trauma due to ramming by the adults. The injuries to the calves are not consistent with other forms of trauma such as boat strike, fisheries interactions, predation, or underwater blasts (Dr. W. McLellan, personal communication, September 2012). Key literature sources include Patterson et al. (1998) and Dunn et al. (2002).

Almost all the quantitative evidence pointing to severe or lethal outcomes for cetaceans arise from ship strikes, particularly strikes of North Atlantic right whales in the Atlantic. Modeling and laboratory efforts have helped to interpret necropsy findings that indicate that lethal encounters are generally the result of forces capable of breaking the whale's jawbone, often the result of multiple microfractures; these models have taken the speed and forces imparted by the ships, as well as the area and time of impact, into account. Controlled laboratory blunt force trauma experiments with pigs yield the closest analogue to marine mammals (Dr. R. Campbell-Malone, Johns Hopkins University, personal communication, month year). Key references include Knowlton and Kraus (2001) and Campbell-Malone et al. (2008).

Captive killer whales tend to avoid stationary objects underwater, so that curiosity is the only likely scenario in which an animal might encounter a turbine. The animals most likely to approach an underwater object are young; older animals are wary. The adults will examine an object but will seldom approach closely. Neonates will be protected by their mothers from harm. The young adolescent orcas, particularly those that do not have a parent nearby, might approach an object. However, the danger from turbines underwater is likely to be small, compared to the risk to these animals from ships moving at speed with high inertia and rotating propellers (Dr. J. McBain, Sea World, personal communication, September 2012).

5.0 Discussion and Conclusions

5.1 Interpretation of Engineering and Biomechanical Analyses

The consequence of tidal turbine blade impact on whale tissue can be roughly estimated from the model data in Table 4 that show that the peak stresses and strains that can be expected from impact from the tidal turbine blade modeled could be 3.750 MPa for the turbine impacting the stationary body of a SRKW, with a 73% elongation of the material, or 2.365 MPa for the impacts with a SRKW swimming toward the turbine with a 93% elongation. These levels of stress are well below what is expected to cause a failure mode in a surrogate material such as natural rubber (10 to 30 MPa) and less than the strain expected to cause rupture of human skin (100%–300%).

Assuming that the SRKW skin can be modeled as a hyperelastic material, the stress-elongation curves in Figure 18 indicate that at the maximum pressure of 3.75 MPa, the response of whale skin would remain in the elastic range. Elongation percentages at the highest turbine blade speed would be in the range from approximately 25% to 200%. At all other blade speeds, elongation would be less. Because the response of these materials is elastic over the range of pressures listed in Table 4, it is expected that if whale skin behaves similarly to these materials, a whale skin tissue would deform and, in conjunction with underlying soft tissue, absorb the force of the strike and would return to normal condition a short time after the pressure was removed. These data indicate that the skin would not be torn by the impact at even the highest exposure pressures.

The published biomechanical properties of blubber indicate that it will react to deformation in a manner similar to that of rubber, displaying properties of deformation that are likely to represent bruising.

Because the engineering analysis considered a whale made entirely of blubber, these results probably represent the worst-case outcome for the soft tissue found below the skin and fibroelastic layers of the SRKW body. This overestimate of potential harm stems from the fact that the skin and associated fibrous layer would probably act as a membrane, distributing the force of the blunt edge blade strike over a larger area of underlying tissue.

Campbell-Malone (2007) provides a value of 17.95 MPa for the ultimate compressive strength for trabecular right whale mandible bone. The ultimate strength for cortical bone is likely to be higher. If this value can be used for killer whale mandibular bone, the highest pressure predicted for turbine blade strike (3.75 MPa) is well below the pressure at which this bone would be expected to fracture. Because the skin and other tissues over the SRKW mandible are likely to absorb most of the pressure from the blade strike, the pressure on the SRKW mandible could be estimated to be an order of magnitude or so below pressures likely to cause fracture.

5.2 Uncertainty of Analyses Outcomes

The overall uncertainty of the engineering and biomechanical analyses can best be estimated by assessing the accuracy of each piece of information that informed the analyses. The modeling techniques used are well documented and are unlikely to have introduced significant uncertainty. Table 9 summarizes the uncertainty of each specific information source. Other parts of the analysis are

conservative, so the conclusions are still conservative, but the uncertainties cannot be further clarified without further study.

Table9. Level of certainty associated with each input to the engineering and biomechanical analyses

Portion of Analysis	Specific Input to Analysis	Accuracy/Level of **Certainty** of Information	Explanation
Modeling of Strike Forces	Geometry of SRKW approach to turbine	High	Geometry of turbine based on detailed drawings from turbine manufacturer; geometry of SRKW based on reports for several SRKWs studied. Chose "worst case for injury" approach of SRKW swimming directly into outer edge of turbine.
	Speed and forces modeled for turbine, as they vary with tidal current speed	High	Turbine speeds and tidal current values are well known, supplied from manufacturer; multiple model runs to determine forces.
	Orientation of animal with turbine blade, transfer of momentum	Medium	Limited model runs for orientation of animal, to ensure choice of "worst case for injury" scenario. Based on engineering judgment.
	Non-linear model for materials	Medium	Does not include model for dermal layers (modeled all-blubber whale) or non-linear model for any materials, leading to overestimate of potential harm to SRKW from turbine.
Biomechanics of orca tissues	Information on tissue thickness and properties of skin	Medium	No direct measures for head of SRKW; information adapted from CT scans of SRKW and literature on other species. Based on professional judgment.
	Information on tissue thickness and properties of blubber	High	Good biomechanical property values from literature to estimate deformation of blubber and transfer of force to underlying tissue & bone.
	Information on tissue thickness and properties of bone	Medium	Biomechanics of impact on bone well understood; used other species in absence of information on SRKW. Based on professional judgment.
	Information on tissue thickness and properties of mellon	Low	Tissue thickness from CT scan and necropsy data, biomechanical values from literature. Properties from blubber used in model because of similar biomechanical properties.
	Effects of blunt force trauma	Medium	Good understanding and copious literature for humans and livestock; little information for marine mammals. Some anecdotal information may be gleaned from interviews. Based on professional judgment.
Sensory response to impact	Post-trauma effects on SRKW	Low	No literature on effects. Potential for anecdotal information from interviews. Not used in model. Other scenarios for different life stages of SRKW and different approaches to the turbine that were not analyzed could create different risks, including

	the potential for delayed effects of head trauma, concussion, injury or death due to infection of lacerations, etc.

5.3 Additional Information to Inform Analyses

In assessing the available blunt force trauma literature, there appears to be is a paucity of data on head injuries in marine mammals that can be associated with reliable estimate of the forces involved. The best available information is associated with whale–ship collisions and, to a lesser extent, data from underwater detonations. Of the available animal surrogate models, the pig provides the most detailed information on head trauma in a large animal model. Recent studies with rodents and in vitro models coupled to some type of computational analysis appear to offer a tractable alternative to traditional animal testing. However, rodent brains react very differently from those of higher mammals, including cetaceans (R. Campbell-Malone, personal communication, September 2012). The information gleaned from the literature may be of value in future marine mammal assessments in which post-mortem (from stranding or other natural cause of death) brain tissue may become available for testing, and more direct measurements of force causing trauma can be made.

Although some interesting insights can be drawn from the anecdotes and professional judgment of veterinarians who care for injured marine mammals and perform necropsies on dead animals, no research is available that directly informs the SRKW interaction with a tidal turbine scenario.

5.4 Next Steps

The engineering and biomechanical analyses reported here indicate that insight can be provided into potential interactions between marine animals and turbines. However, it is clear that the information base of mechanical properties for marine mammal tissues lacks key pieces critical to the analyses. We propose the collection of an enhanced database of marine mammal biomaterial properties. This information could be collected through a coordinated action to recover more biomechanical information on marine mammal tissue and bone as a routine part of the existing necropsies on animals found dead. Also of importance are data on specific properties and operational modes of turbines that could cause harm to marine animals; for example, material properties that can be used on the leading edges of turbine blades to decrease potential harm to animals. Animal models are needed that can connect the biomechanical properties of marine mammals and design criteria for turbines, allowing for a modeling application to evaluate the design of turbines before deployment.

It is also important to note that the analyses performed here do not necessarily inform interactions between tidal turbine blades from devices with designs different from those of the open center OpenHydro turbine, nor are these analytical outcomes necessarily transferable to turbine blade interactions with other marine mammals. We propose that analyses of additional turbine designs, interacting with other marine mammals potentially at risk, be performed. Of particular interest are studies that link turbines with unducted blades and vertical axis turbines with marine mammals that differ in size, body conformation, and mass from those of the adult SRKW.

5.5 Conclusion

Little is known about the potential effects of tidal turbine blade impacts on SRKW; the engineering and biomechanical approach in this study demonstrates that insight can be provided, even in the absence of definitive data. A SRKW interaction with a turbine in 55 m of water in Admiralty Inlet is unlikely, as SRKWs spend 97% of their time at 30 m or higher. In the rare occurrence of a whale strike, modeling the speed and potential force exerted by an OpenHydro tidal turbine blade allowed SNL to estimate the maximum force of tidal turbine blunt edge blades acting upon soft tissue and bone of a SRKW. The SRKW modeled in the finite element model was composed of a single layer of tissue, essentially a whale made entirely of blubber. This structure introduces a conservative element to the outcome, as the skin of the SRKW is more resistant to injury and would distribute the force from the blade. In the real world, the forces from a tidal turbine blade strike that might cause injury to the "all blubber" whale will cause less damage to the living animal. Further, the engineering model used the maximum speed for the turbine blades and whale swimming speed, making this analysis an extreme scenario. Coupled with PNNL's biomechanical analysis of whale blubber and tissue, the model provided a basis for assessing the potential injury to a SRKW. A review of existing literature and interaction with marine veterinarians experienced with injured marine mammals did not elucidate the outcome greatly.

The PNNL and SNL analyses determined that an adult male SRKW weighing approximately 4,000 kg is not likely to experience significant tissue injury from impact by an OpenHydro tidal turbine blade in the configuration used in this analysis. Based on a number of assumptions, SRKW skin and the underlying soft tissue should absorb the force of the strike without external damage to the skin or fracturing of the mandibular bone. However, key information required to fully understand the biomechanical properties of marine mammal tissues is lacking, limiting the results of the analyses. To address the lack of data, conservative estimates were made, and the worst-case scenario was used for the modeling studies. The addition of improved biomechanical data could improve the conclusions reached by these analyses.

6.0 References

Baird RW, MB Hanson, EE Ashe, MR Heithaus, GJ Marshall. 2003. Studies of foraging in "southern resident" killer whales during july 2002: dive depths, bursts in speed, and the use of a "crittercam" system for examining sub-surface behavior. National Marine Fisheries Service, National Marine Mammal Laboratory, Seattle, Washington.

Campbell-Malone R. 2007. Biomechanics of north atlantic right whale bone: mandibular fracture as a fatal endpoint for blunt vessel-whale collision modeling, Massachusetts Institute of Technology, Woods Hole Oceanographic Institution, Woods Hole, Massachusetts.

Campbell-Malone R, SG Barco, PY Daoust, AR Knowlton, WA McLellan, DS Rotstein, MJ Moore. 2008. Gross and histologic evidence of sharp and blunt trauma in north atlantic right whales (eubalaena glacialis) killed by vessels. *Journal of Zoo and Wildlife Medicine* 39(1):37-55.

Dunn DG, SG Barco, DA Pabst, WA McLellan. 2002. Evidence for infanticide in bottlenose dolphins of the western north atlantic. *Journal of Wildlife Diseases* 38(3):505-510.

Durban J, H Fearnbach, D Ellifrit, and K Balcomb. 2009. Size and body condition of Southern Resident Killer Whales. Contract report to the Northwest Regional Office, National Marine Fisheries Service. Order number AB133F08SE4742, Requisition Number NFFP5000-8-43300.

Hanson, MB. 2001. An evaluation of the relationship between small cetacean tag design and attachment durations: a bioengineering approach. Ph.D. dissertation, Univ. of Washington, Seattle, WA. 208 pp.

Hendriks FM. 2001. Mechanical behavior of human skin in vivo, a literature review. Report 2001/820, Koninklijke Philips Electronics, N.V. Amsterdam, the Netherlands.

Kipps EK, WA McLellan, SA Rommel, DA Pabst. 2002. Skin density and its influence on buoyancy in the manatee (*trichechus manatus latirostris*), harbor porpoise (*phocoenca phocoaena*), and bottlenose dolphin (*tursiops trucnatus*). *Marine Mammal Science* 18(3):765-778.

Koteras JR, AS Gullerud, NK Crane, and JD Hales. 2006. *Presto User's Guide Version 2.6*. SAND2006-6093, Sandia National Laboratories, Albuquerque, New Mexico.

Lightsey JD, SA Rommel, AM Costidis, TD Pitchford. 2006. Methods used during gross necropsy to determine watercraft-related mortality in the florida manatee (*Trichechus manatus latirostris*). *Journal of Zoo and Wildlife Medicine* 37(3):262-275.

McKenna MF. 2005. *Comparative morphology of the odontocete melon: Functional and evolutionary interpretations*. Masters of Science thesis, San Diego State University, San Diego, California.

Noren DP. 2011. Estimated field metabolic rates and prey requirements of resident killer whales. *Marine Mammal Science* 27(1):60–77.

Oremland, M.S. and B.M. Allen. 2010. Mandibular fractures in short-finned pilot whales, *Globicephala macrorhynchus.* Marine Mammal Science 26(1): 1–16.

Patterson IA, RJ Reid, B Wilson, K Grellier, HM Ross, PM Thompson. 1998. Evidence for infanticide in bottlenose dolphins: an explanation for violent interactions with harbour porpoises? *Proceedings of the Royal Society - Biological Sciences* 265(1402):1167-1170.

Rommel SA, AM Costidis, TD Pitchford, JD Lightsey, RH Snyder, EM Haubold. 2007. Forensic methods for characterizing watercraft from watercraft-induced wounds on the florida manatee (*Trichechus manatus latirostris*). *Marine Mammal Science* 23(1):110-132.

Schaefer RJ. 2009. Mechanical Properties of Rubber. In *Harris' Shock and Vibration Handbook* (5th edition). AG Piersal and TL Paez (eds), pp 1108-1125. McGraw Hill, New York.

Silver FH, JW Freeman, and D DeVore. 2001. Viscoelastic properties of human skin and processed dermis. *Skin Research and Technology* 7(1):18–23.

Soldevilla MS, MF McKenna, SM Wiggins, RE Shadwick, TW Cranford, and JA Hildebrand. 2005. Cuvier's beaked whale (*Ziphius cavirostris*) head tissues: physical properties and CT imaging. *Journal of Experimental Biology* 208:2319–2332.

Tsukrov I, JC DeCrew, K Baldwin, R Campbell-Malone, MJ Moore. 2009. Mechanics of the right whale mandible: full scale testing and finite element analysis. *Journal of Experimental Marine Biology and Ecology* 374(2):93-103.

Williams R, DP Noren. 2009. Swimming speed, respiration rate, and estimated cost of transport in adult killer whales. *Marine Mammal Science* 25:327-350.

Winn JP. 2006. *Modeling Large Whale Entanglement Injuries: An Experimental Analysis of the Influence of Tissue Compliance, Line Tension, and Draw-Length on Epidermal Abrasion Resistance.* Masters of Science thesis, University of Maine, Orono.

Winn JP, Woodward B, Moore MJ, Peterson ML. 2008. Modeling whale entanglement injuries: An experimental study of tissue compliance, line tension, and draw-length. *Marine Mammal Science* 24: 326-340.

Prepared for the U.S. Department of Energy
under Contract DE-AC05-76RL01830

This report prepared in partnership with Sandia National Laboratories

Pacific Northwest
NATIONAL LABORATORY

Proudly Operated by **Battelle** *Since 1965*

Sandia
National
Laboratories

902 Battelle Boulevard
P.O. Box 999
Richland, WA 99352
1-888-375-PNNL (7665)
www.pnnl.gov